AFRL-VS-HA-TR-2004-1038

DIAGNOSTICS AND MODELING OF THE AURORAL IONOSPHERE UNDER THE INFLUENCE OF THE GAKONA HF TRANSMITTER

Davis D. Sentman
Eugene M. Wescott
John V. Olson
Antonius Otto
William A. Bristow
Daniel J. Solie
John K. Petersen

Geophysical Institute
University of Alaska Fairbanks
903 Koyukuk Drive
Fairbanks, AK 99775-7230

27 February 2004

Final Report

20040730 033

AIR FORCE RESEARCH LABORATORY
Space Vehicles Directorate
29 Randolph Rd
AIR FORCE MATERIEL COMMAND
Hanscom AFB, MA 01731-3010

This technical report has been reviewed and is approved for publication.

/Signed /

_____
JAMES C. BATTIS
Contract Manager

/Signed /

_____
ROBERT A. MORRIS
Branch Chief

REPORT DOCUMENTATION PAGE

The public reporting burden for this collection of information is estimated to average 1 hour per response, including the time for reviewing instructions, searching existing data sources, gathering and maintaining the data needed, and completing and reviewing the collection of information. Send comments regarding this burden estimate or any other aspect of this collection of information, including suggestions for reducing the burden, to Department of Defense, Washington Headquarters Services, Directorate for Information Operations and Reports (0704-0188), 1215 Jefferson Davis Highway, Suite 1204, Arlington, VA 22202-4302. Respondents should be aware that notwithstanding any other provision of law, no person shall be subject to any penalty for failing to comply with a collection of information if it does not display a currently valid OMB control number.
PLEASE DO NOT RETURN YOUR FORM TO THE ABOVE ADDRESS.

1. REPORT DATE (DD-MM-YYYY)	2. REPORT TYPE	3. DATES COVERED (From - To)
27 -02- 2004	Final Report	July 29, 1999 to August 31, 2003

4. TITLE AND SUBTITLE

Diagnostics and Modeling of the Auroral Ionosphere
under the influence of the Gakona HF Transmitter

5a. CONTRACT NUMBER
F19628-99-C-0059

5b. GRANT NUMBER

5c. PROGRAM ELEMENT NUMBER
62601F

6. AUTHOR(S)
Sentman, Davis D.
Wescott, Eugene M.
Olson, John V.
Otto, Antonius
Bristow, William A.
Solie, Daniel J.
Petersen, John K.

5d. PROJECT NUMBER
4266

5e. TASK NUMBER
GH

5f. WORK UNIT NUMBER
AJ

7. PERFORMING ORGANIZATION NAME(S) AND ADDRESS(ES)
Geophysical Insititute
University of Alaska Fairbanks
903 Koyukuk Drive
Fairbanks, AK. 99775-7230

8. PERFORMING ORGANIZATION REPORT NUMBER

9. SPONSORING/MONITORING AGENCY NAME(S) AND ADDRESS(ES)
Air Force Research Laboratory
29 Randolph Road
Hanscom Air Force Base, MA 01731-3010
Contract Manager: James Battis, VSBX1

10. SPONSOR/MONITOR'S ACRONYM(S)

11. SPONSOR/MONITOR'S REPORT NUMBER(S)
AFRL-VS-HA-TR-2004-1038

12. DISTRIBUTION/AVAILABILITY STATEMENT
Approved for public release; distribution unlimited

13. SUPPLEMENTARY NOTES

14. ABSTRACT

This Final Report covers the activities and results of the subject contract during the period 29 July, 1999 to 31 August, 2003. The concept underlying the research was to investigate the manner in which the Gakona HF Transmitter interacts with the ionospheric D-region, and by means of a number of experiments and theoretical models to characterize the resultant effects. A Public Outreach program was instituted to help educate the community in the Gakona area about the goals and research of the HAARP program. The work in the contract was divided into 5 subtasks, each under the direction of a separate UAF investigator: 1. ELF/VLF Wave Measurement and Interpretation Program (D. Sentman), 2. ULF Wave Measurement Program (J. Olson), 3. Simulation (A. Otto), 4. SuperDARN Operations (W. Bristow), and (5) Public Outreach (D. Solie). These subtasks are described in their respective Sections.

15. SUBJECT TERMS
HAARP, Ionosphere, Diagnostics, Modeling

16. SECURITY CLASSIFICATION OF:			17. LIMITATION OF ABSTRACT	18. NUMBER OF PAGES	19a. NAME OF RESPONSIBLE PERSON
a. REPORT	b. ABSTRACT	c. THIS PAGE	SAR	42	James Battis
unclassified	unclassified	unclassified			**19b. TELEPHONE NUMBER** (Include area code) 781-377-4669

CONTENTS

FIGURES

TABLES

ACKNOWLEDGEMENTS

SYMBOLS, ABBREVIATIONS, ACRONYMS

AMT	**Audio Magneto Telluric**
CIGO	**College of International Geophysics Observatory (UAF and Kaktovik)**
CSAMT	**Controlled Source Magneto Telluric**
CV	**Copper Valley**
CVS	**Copper Valley Schools**
MHD	**Magnetohydrodynamics**
MSIS	**Mass Spectrometer Incoherent Scatter (model)**
NCAR	**National Center for Atmospheric Research**
PEJ	**Polar Electrojet**
PWSCC	**Prince William Sound Community College**
SEE	**Stimulated electromagnetic emissions**
SuperDARN	**Super Dual Auroral Radar Network**
TIME-GCM	**Thermosphere ionosphere mesosphere electrodynamics general circulation model**
UAF	**University of Alaska Fairbanks**
ULF	**Ultra-low frequency**
UT/UTC	**Universal Time**
ULF	**Ultra-low frequency**
WISE	**Wrangell Institute for Science and the Environment**

1. ELEMENT 1: ELF/VLF WAVE MEASUREMENT AND INTERPRETATION PROGRAM

1.1 Summary

The overall objective of Element 1 is to establish the characteristics of the ionospheric source region responsible for the ELF/VLF waves generated by modulation of HAARP HF emissions. To accomplish this objective we established two sub-objectives. The first was to construct ELF monitoring capabilities over the passband of interest to HAARP studies, generally 5-10,000 Hz, at two base or reference sites for routine experimenter use during and between campaigns. The second was to measure the ELF radiation pattern. The first sub-objective and the observational and preliminary interpretation components of the second sub-objective were met during the period of the contract.

1.2 Introduction

We describe first the ELF facilities and instruments to monitor the effects of HF modulation of the Polar Electrojet (PEJ) at ELF and VLF frequencies. This is followed by a description of the Fall 2000 campaign to measure the radiation pattern, and results of the preliminary analysis of the observations.

1.3 The Gakona and Poker Flat ELF Systems

1.3.1 Methods, Assumptions and Procedures

The measurements are made at two locations. One site close (~10 km) to HAARP, is located north of Gakona Junction and used to monitor the near field ELF/VLF emissions. A second site is located at the Poker Flat Research Range, north of Fairbanks at a distance of ~350 km from HAARP. These systems were developed to give HAARP experimenters easily accessible ELF monitoring capabilities and for baseline signal levels for comparison with other remote measurements.

The two systems are configured to be as close to identical as possible. The sensors at each site are electrostatically shielded induction coils (EMI, Inc., model BF-10) optimized for operation in the frequency band 3-12,000 Hz. They are installed horizontally along geographic North/South and East/West axes and measure the orthogonal horizontal components of the magnetic field. Sensor outputs are delivered via optical fiber to a real-time data acquisition and analysis system. Figure 1 shows the sensors and instrument trailer at Gakona. The real time computer systems convert the signals to digital form at 27.8 kHz using GPS synchronization, and perform various signal conditioning and filtering operations, and compute a variety of diagnostic information. These include synchronous detection of HAARP modulation frequencies, waveform stacking, and dynamic frequency-time spectra and amplitude distributions. The system is also used as a development test bed for new detection and analysis methods. The system can be remotely configured and administered over the Internet. The basic characteristics of the Gakona and Poker Flat systems are given in Table 1.
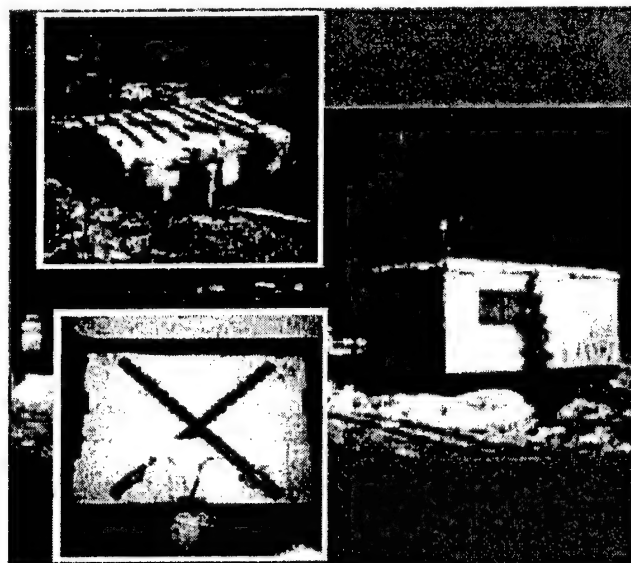
Figure 1. Sensors, Sensor Box, and Instrument Trailer at Gakona ELF Site.

Table 1. Analog System (Basic Characteristics of Gakona and Poker Flat Systems)

Analog System

	Component	Description
•	Sensors	EMI BF-10 Induction Coils, 3-12000 Hz, sensitivity ~1 pT-Hz$^{-1/2}$
•	Receiver Hardware	Multi-stage: Analog sensor-preamplifier close to sensors; 20-bit, 48 kHz sampling for fiber optic transfer of signals to primary receiver/amplifier.
		DSP 16-bit, 44.1 kHz sampling for 60 Hz rejection comb filter
		12-bit, 27.777 kHz sampling for computer analysis and recording
•	Time Standard	Spectrum Time Machine GPS, ~1 microsec accuracy absolute

Table 2. Data Acquisition System (Basic Characteristics of Gakona and Poker Flat Systems)

Data Acquisition System

	Component	Description
•	Digital Platform	PC, 350 MHz Pentium II
•	OS	Microsoft Windows NT 4.0 Server
•	A/D Subsystem	Data Translation DT-3001 12-bit ADC/DAC/CTR; external triggering from 1 MHz TTL GPS source
•	Network	Ethernet, TCP-UDP/IP
•	Software Architecture	Client-server; real-time data server feeding client analysis modules
•	Data Base Format	NetCDF, HAARP conventions
•	Remote Control	Various; principally NetMeeting and pcAnywhere

Table 3. Software Modules (Basic Characteristics of Gakona and Poker Flat Systems)

Software Modules

Module	Function	Status
• Data Server	Sample data at 27.777 kHz from down-counted 1-MHz TTL external GPS source; sampled signal low pass filtered and subsampled into 4 user- selectable filter banks. Matlab 5.3 libraries extensively for FFT, IIR filtering operations.	Operational
• Synchronous Detection	Detect and log amplitude and phase of narrow band signals; up to 14 user specified signal and 8 noise frequencies in band pass 3-10000 Hz, with absolute phase stability < 1 microsec; arbitrarily long integration intervals; linear and non-linear detection options	Operational
• Spectra	Compute and log dynamic spectra 3-200 Hz	Operational
• Time Series	Log sampled, time stamped data from any of 4 filter banks	Operational
• Q-Burst	Detect and log ELF transients	Operational
• Amplitude Probability Distributions	Assemble and log amplitude probability distributions; used as input to non-linear option of synchronous detection module	Preliminary tests
• Stack	Assemble and log stacked periodic waveforms of arbitrary period	Operational
• Multisite	Differential measurements between widely separated stations, long base lines.	Preliminary tests

In establishing these systems, numerous engineering difficulties were isolated and removed. An absolute calibration procedure was developed to provide end-to-end amplitude and phase response of the ELF receiver systems over the passband 3-Hz to 10 kHz.

An example of results obtained from the Gakona ELF system during the Fall 2000 campaign is shown in Figure 2.

1.3.2 Antenna Pattern Measurements

1.3.2.1 Preliminary site survey

A set of field measurements were made at various distances and azimuths from HAARP in order to characterize the antenna pattern. The instruments used for the field observations were Zonge Engineering (Tucson, AZ) ELF induction coils operating with the model GDP 32 II data recorder system. The equipment permitted using HAARP as a controlled source in a series of controlled source magneto telluric (CSAMT) resistivity vs. depth measurements. The Zonge equipment was modified to operate within the parameter regime required for the field measurements, and arrived in time for preliminary tests during the HAARP June/July 1999 campaign.
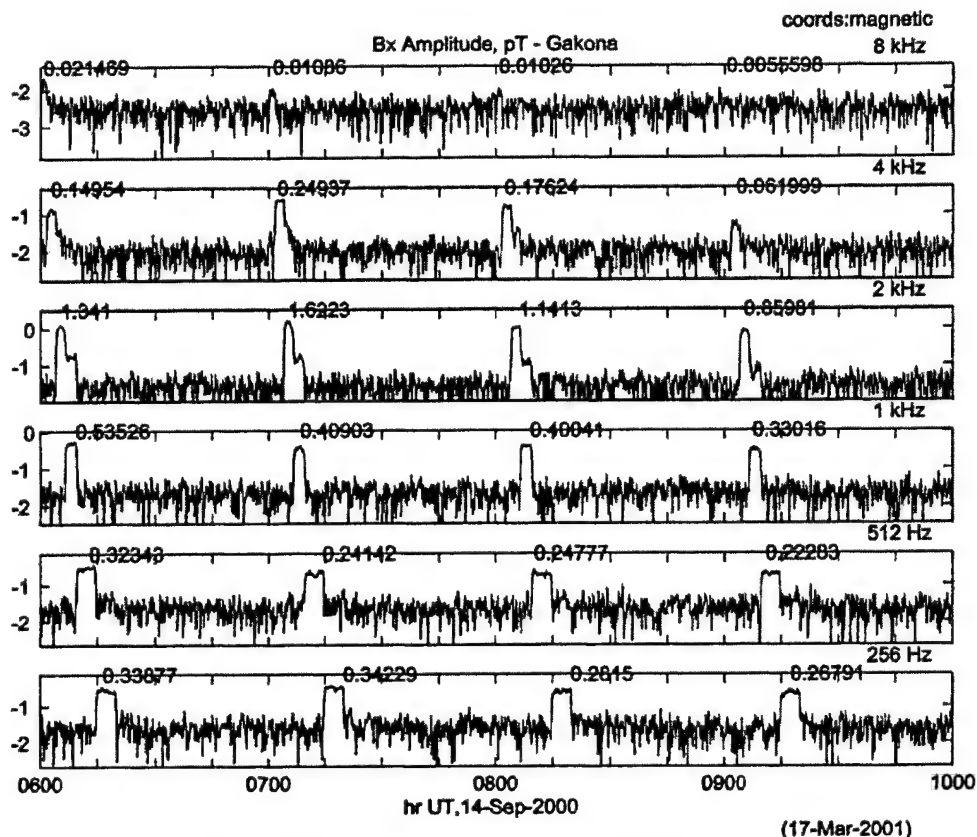
Figure 2. Synchronously Detected Signals 256-4000 Hz in Bx in During the Fall 2000 Campaign.

Observations were first made from the site near a capped wildcat well; Tazlina #1 located about 75.6 km from HAARP on Lake Louise Road, for which logs exist. On the night of 2 July 1999 the first successful observations were obtained over frequencies at powers of 2 from 4 Hz to 8192 Hz, and very strong signals were received.

The HAARP signal apparent resistivity vs. frequency obtained from these tests is shown in Figure 3. Some minor smoothing was required for a few points. The results from the Ey/Hx apparent resistivity are shown in the figure. The resistivity log from Tazlina #1 starts at a depth of 340 m, because the well was cased to that depth, so we cannot compare the log and the CSAMT data directly. The logged resistivity starting at 340 m is almost constant 5 ohm-m in reasonable agreement with our deepest values. The obvious sediments near the surface at the site are well-rounded river sediments and silts compatible with the 20 to 25 ohm-m values measured with the CSAMT closest to the surface.

During the September/October 1999 HAARP campaigns, additional measurements were made at several sites to test our equipment and analysis techniques that were subsequently used for the antenna pattern survey and characterization. We successfully measured two components of H and the corresponding E fields at a site 50 km from HAARP at frequencies: 16, 32, 64, 128, 256, and 512 Hz. The analysis of the data used a modified version of software used in the synchronous detection modules of the Gakona and Poker Flat systems. Following this successful test, plans were made to obtain three specially modified data loggers for the full antenna pattern measurement campaign in the spring of 2000.

4

1.3.2.2 Sites for antenna pattern measurements

In June 1998 a preliminary survey was conducted of sites at 50, 100, and 200 km distance from HAARP to determine the suitability of 12 sites, as the minimum we would need in the survey. At each site we used the natural electromagnetic noise from the ionosphere in the audio magneto telluric (AMT) method to determine the background noise spectrum and the ground resistivity vs. frequency. We also measured 60 Hz power line and harmonics noise for interference. Likely sites at 150 km distance were also located, but due to shortage of time were not measured for magneto telluric resistivity.

Following the summer 1999 preliminary field survey, we expanded the number of remote measurements systems to include three leased Zonge systems in addition to the existing one, for a total of four. This would permit making measurements from four sites simultaneously. With this scheme it was decided to use the four systems distributed approximately in four quarters on circles centered on HAARP at distances of 50, 100, 150 and 200 km. The University of Alaska Maps Office selected a suite of likely sites, and the University Office of Land Management sought permission for temporary use of the land to make the measurements. The land was owned by various owners or managers: U.S. Forest Service, U.S. Bureau of Land Management, State of Alaska, and Ahtna Native Corporation, and various native village corporations. Figure 4 shows the sixteen remote sites actually used in the HAARP survey, plus the site at Gakona. The natural source AMT measurements could be used to compare with the results calculated from the ratios of the electric and magnetic components of the HAARP signals.
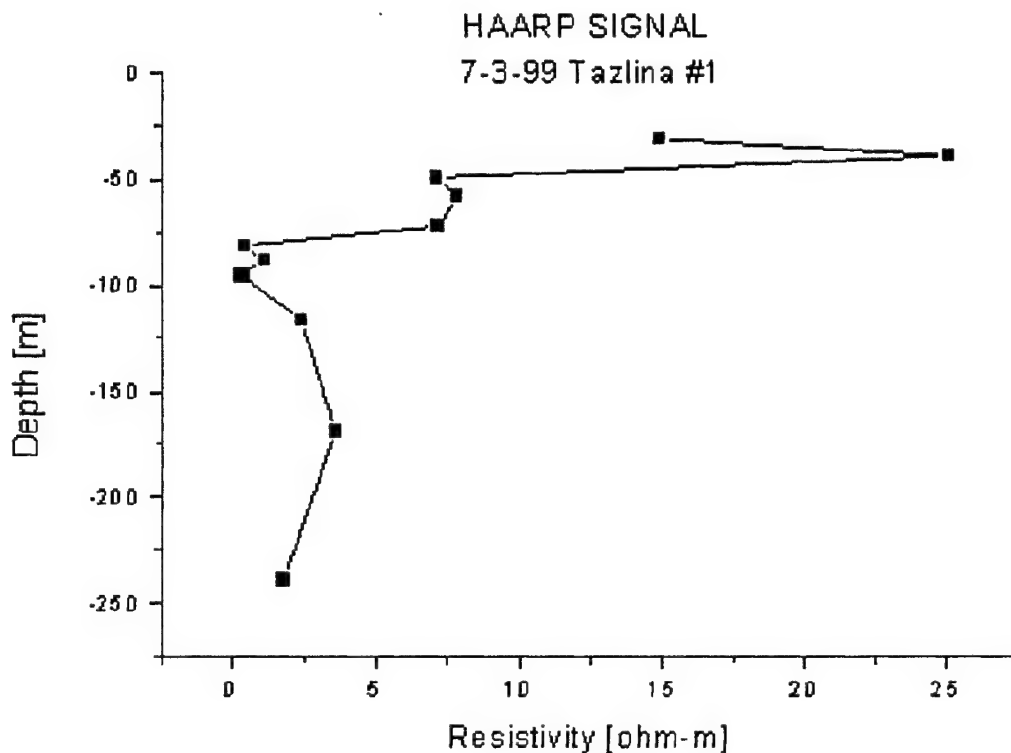
Figure 3. Resistivity vs. Depth Calculated Using the Bostick Algorithm Derived from the Modulated HAARP Signal.

Figure 4. Remote Field Sites Used for Antenna Pattern Measurements, Plus the Gakona Reference Site (GAK) and the HAARP Location (HAARP). The Legend at the Right Refers the Site Designations to Their Names.

In order to make the necessary two-component B field measurements to determine the HAARP antenna pattern, we first experimented with a Zonge Engineering data recording system and coils purchased for the project. The GDP-32 II is a multi-channel receiver designed to acquire virtually any type of electromagnetic or electrical data within the DC to 8 kHz bandwidth. It is waterproof and portable. The time base is an oven-controlled oscillator with 5×10^{-10} per 24 hours aging rate. The system was equipped with GPS-disciplining for greater timing control. The two Zonge coils have a flat response of 100 mV/nT over the frequency range of interest.

1.4 Results and Discussion

1.4.1 Fall 2000 Campaign

Permission for an extended field campaign in September 2000 was obtained from all the pertinent landowners, and a contract was let for the lease of three Zonge GDP 32-II data loggers and magnetometer coils. All the antenna pattern field measurements were carried out by four crews operating from four rented motorhomes to provide accommodations at the remote field sites. They were equipped with generators for providing 60 Hz power for recharging batteries and transferring the data to digital tape. In order to reach the 200 km distance site about 40 miles from Cordova, a charter aircraft was flown from Valdez.

The field campaign began on 5 September 2000 with measurements of both E and H components at four sites each 50 km distant from HAARP. Observations at each site continued on successive nights until the HAARP magnetometer coils at Gulkana indicated strong signals.

6

Excellent data were obtained on the UT nights of 7 September at 50 km, 8 September at 100 km, 12 September at 150 km and 14 September at 200 km distances. The very best night of ELF/VLF activity occurred on the night of 14 September. The data from the four nights at the four distances, have been spectrally analyzed and it is clear that excellent data were obtained at all distances out to 200 km from HAARP. The frequency range with good data includes 4, 8, 16, 32, 64, 128, 256, 512, 1000, 2000 and 4000 Hz

All the field data were copied from the digital tapes to the DVD-RAM format, with a spare set recorded for backup. Sample data from each night, at each site, were spectrally analyzed to determine the quality of the data obtained from each of the sixteen sites. The frequency range with good data includes 4, 8, 16, 32, 64, 128, 256, 512, 1000, 2000, and 4000 Hz at all distances out to 200 km The total sampled data for the campaign comprised approximately 40 GB.

1.4.2 Data Analysis

Several kinds of data analyses were performed on the observations.

1.4.2.1 Amplitude and phase of HAARP-generated modulation signals

The data from each site comprised signals sampled at 4096/sec. Amplitude calibrations for each of the electric and magnetic channels were applied to the data to produce absolute signal levels. From these sampled data the amplitude and phase were computed for each of the individual frequencies 4, 8, 16, 32, 64, 126, 256, 1000, and 2000 Hz. Figure 5 shows sample results 256-4000 Hz for the By channel obtained from Cordova on 14 September 2000. Figure 6 shows the corresponding results for the Ex channel.
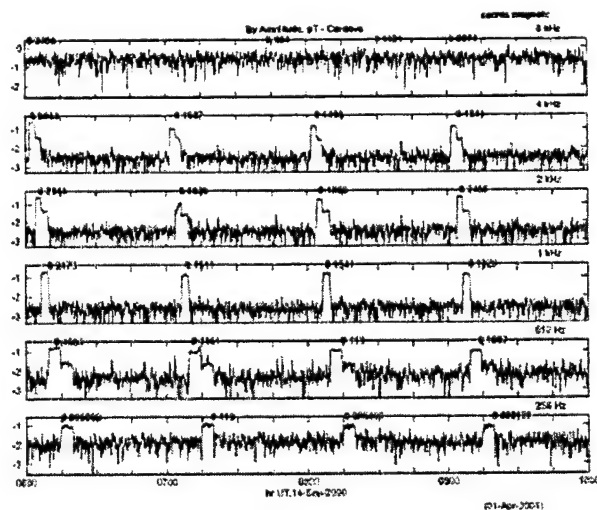
Figure 5. Amplitude in pT of the By Magnetic Component of Synchronously Detected HAARP Signals Obtained 14 Sep 2000 from Cordova, 200 km from HAARP. The Vertical Scale is Logarithmic, and is in Absolute Units. Amplitudes of the Maximum Signal are Printed at the Various Peaks.
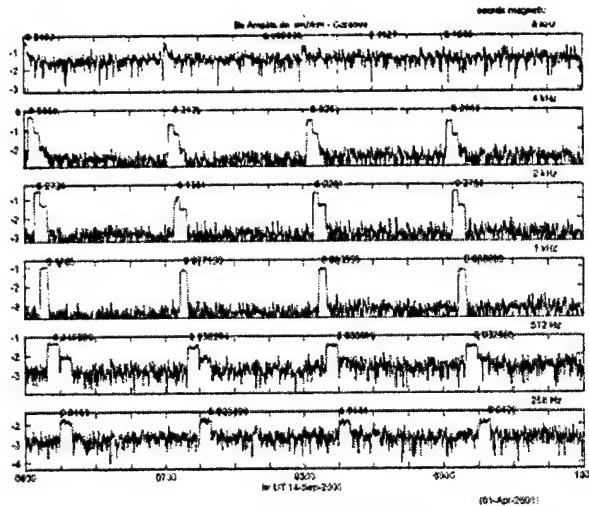
Figure 6. Amplitude in mV/km of the Ex Electric Component Corresponding to Figure 5.

7

1.4.2.2 Preliminary interpretation

Amplitude and phase calculations were performed on all data. The results were analyzed by Peter Bannister to produce a preliminary model of the radiation pattern based on the observed amplitudes and phases at the measurement sites.

The basic ionospheric model is shown in Figure 7. In this preliminary model the ionosphere is assumed to be a homogenous slab of constant conductivity 3×10^{-5} S/m, with a base at altitude h. The perturbed electrojet is assumed to create a horizontal magnetic dipole with moment m A/m^2.

The analytic expressions used to represent electric and magnetic field components at the ground are given in Appendix A. The adjustable parameters in this model are the ionospheric conductivity, the dipole magnitude m, its height h and its orientation ϕ. The equivalent image line dipole model is shown in Figure 8. By adjusting the model parameters, a good fit was obtained to the simultaneous measurements at each of the remote sites. Figure 9 shows an example of the quality of the fit obtained between the observations made at the Gakona base site and Sutton, 210 km west of HAARP and the model. The data indicate the effective height of the magnetic dipole was at 91.5 km, and had a moment of 3.1×10^9 A-m^2. The orientation was magnetic north south. For this particular run the magnetic amplitudes were maximum at 2 kHz at Gakona, at a value of ~3 pT. The corresponding value at Sutton was ~0.5 pT. Similar analyses were performed for each of the other stations for each of the nights on which good signals were obtained. The resulting ionospheric dipole model yields intensity maps as functions of frequency and position for distances to ~300 km from HAARP. Figures 10 and 11 show model intensity maps for 4 Hz and 1 kHz based on based on fits for the height of the dipole moment. They are normalized to 0 dB at HAARP. Of interest in these maps is the existence of nulls at magnetic north-south distances from HAARP of ~100 km.

1.4.2.3 Polarization

The elliptical polarization parameters were extracted from the amplitudes and phases of the orthogonal horizontal components of the magnetic and electric fields. These parameters are useful in separating time varying effects of the anisotropic ionosphere from effects induced by anisotropies in the local ground conductivity. Examples of polarization parameters derived during two nights exhibiting both left-hand (LH) and right-hand (RH) polarizations, respectively, are shown in Figures 12 and 13.

1.5 Conclusions

A preliminary report with the results shown here was presented at the RFII Meeting in Santa Fe in May 2001. These results are based on modeling the amplitudes as measured at each of the various sites. A more complete analysis that makes use of the vector measurements and polarization properties has been initiated and continues.
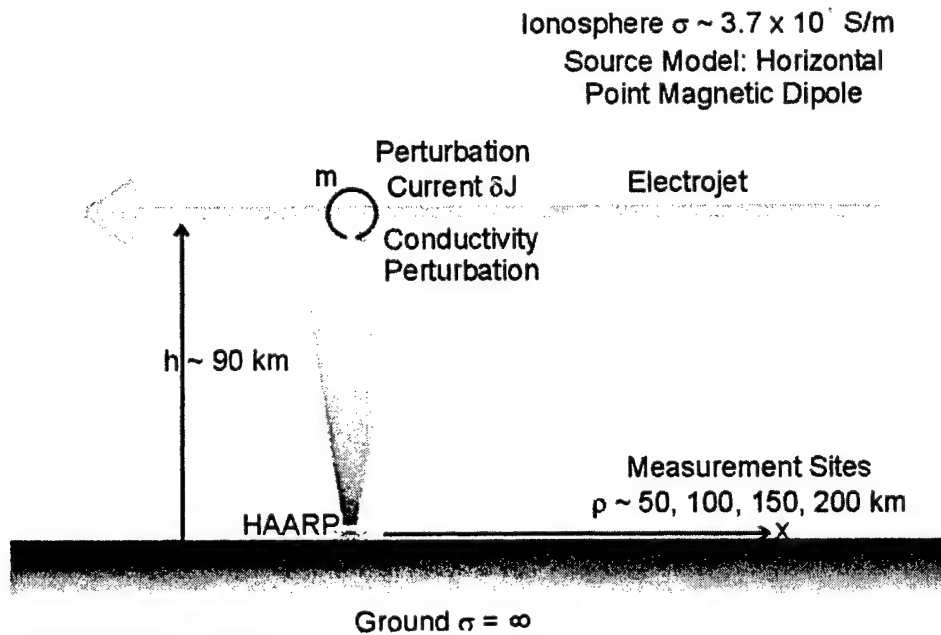
Figure 7. Basic Geometry of Earth-Ionosphere Model Showing HAARP RF Beam and Horizontal Magnetic Dipole at the Base of the Ionosphere.
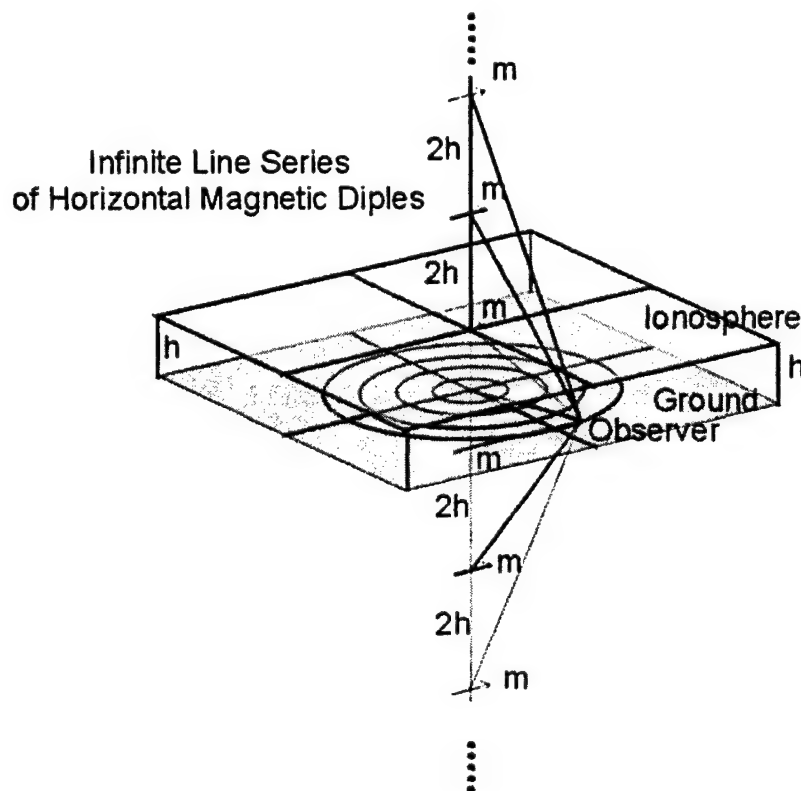
Figure 8. Equivalent Set of Image Line Dipoles Used to Compute the Antenna Pattern.

9
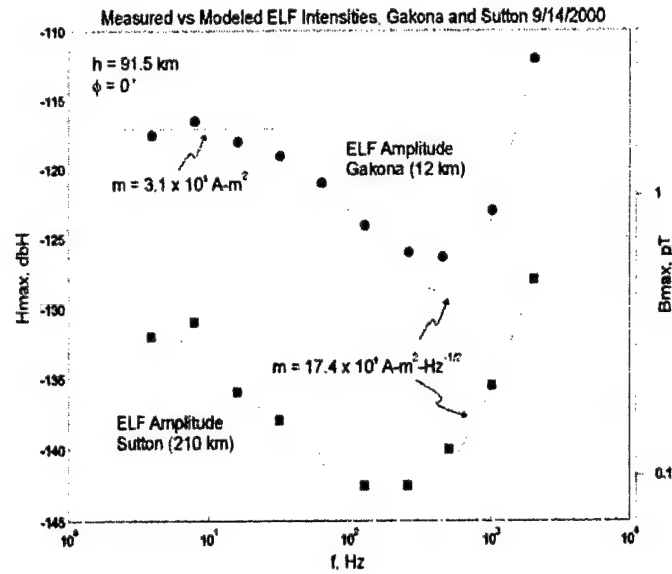
Figure 9. Comparison of Measured ELF Amplitudes at Gakona and Sutton (Solid Dots) with Model Amplitudes. The Amplitude Scale at the Left is in dBH, and at the Right pT.
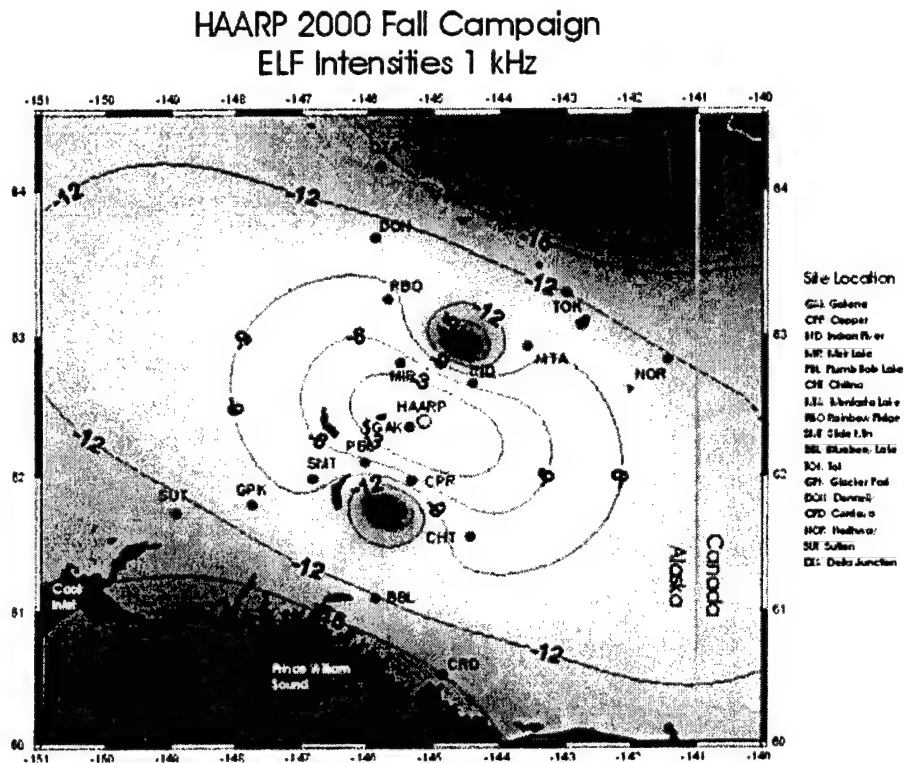
Figure 10. Grayscale Model Amplitude Distribution of ELF Radiation from HAARP at 1 kHz. The Intensity is Normalized to 0 dB at HAARP. Contours of Constant Amplitude are Drawn at 3 dB Intervals.

10
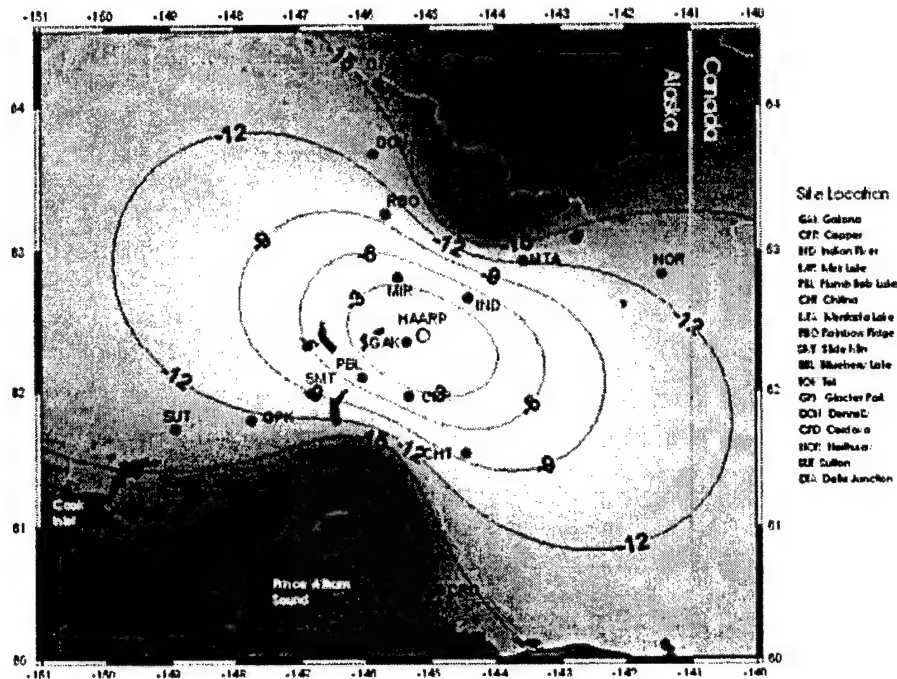
Figure 11. Model Amplitude Distribution of ELF Radiation from HAARP at 4 Hz.
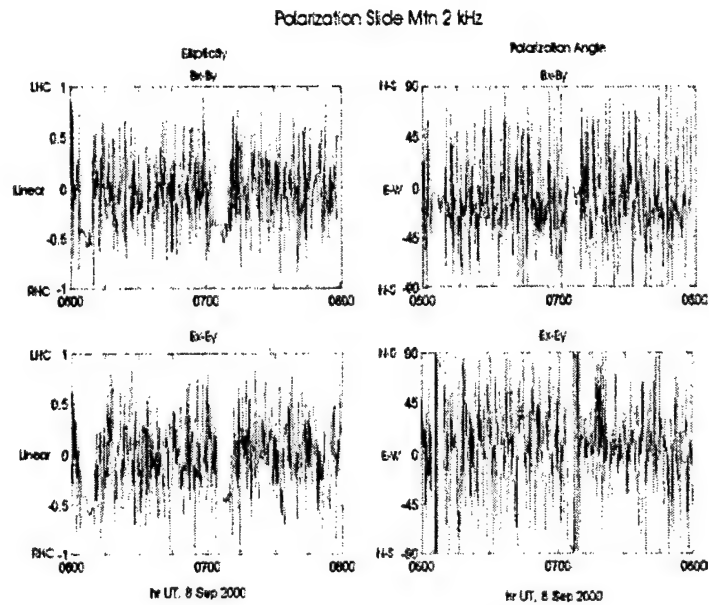
Figure 12. Ellipticity Parameters for Two Intervals of Strong LH ($e \sim -0.5$) Elliptical Polarization at the Slide Mountain Site, 14 Sep 2000.

11
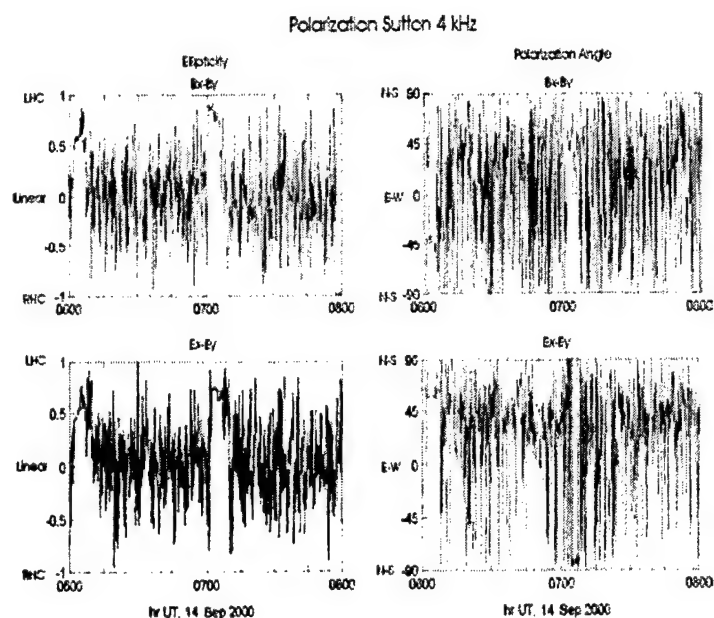
Figure 13. Ellipticity Parameters for Two Intervals of Strong RH ($e \sim +0.6$) Elliptical Polarization at the Sutton Site, 14 Sep 2000.

1.6 Recommendations

The fieldwork that went into obtaining the results obtained above involved considerable expenditure of manpower and effort, and the resultant data set was very large. Continuing work is being performed to reduce and extract additional information from the data that goes beyond the simple characterization of the ionospheric source function in terms of magnetic dipole moment and height given here. If it turns out that the basic characterization of the ionospheric source region involves only a small number of parameters, such as the magnitude, height and orientation of the magnetic dipole moment, as we have assumed here, then systematic monitoring of these parameters should be possible using a much smaller number of field sites than the 17 that we used in our studies.

2. ELEMENT 2: ULF WAVE MEASUREMENT PROGRAM

2.1 Summary

The purpose of our experiment was to attempt to stimulate hydromagnetic waves in the ionospheric wave-guide using the HAARP heater. A wave-guide exists in the Earth's ionosphere due to the maximum charge density located in the F-Region. This 'duct' allows natural ULF pulsations in the 0.1–5 Hz band to propagate across large horizontal distances from the source location.

Ionospheric wave-guide theory tells us that two wave modes can exist in the duct, coupled by the Hall conductivity. We have hypothesized that modulated heating of the ionosphere can cause a variation in the Hall current that will serve as a source of ULF waves. We have employed two induction magnetometers, operated by the Geophysical Institute at College and Kaktovic, Alaska, to detect the ULF signals that are produced in the duct.

The experiment was run three times and we were not successful in stimulating detectable signals. While we have evidence that the duct was present during our earlier runs and that our instruments are sensitive enough to detect any signals generated, we do not know the topology of the currents generated by the heater. If the current patterns are complex there may not be a significant amount of radiation produced. A better analysis and understanding of the heated region along with a more detailed theoretical experimental basis is needed for further trials.

2.2 Introduction

2.2.1 Background

2.2.1.1 The ionospheric wave-guide

As a consequence of the variation in electron and ion densities in the ionosphere, the index of refraction for low-frequency electromagnetic waves that can propagate in the ionospheric plasma also varies. The phase speed of these waves, termed the Alfven speed, is proportional to the inverse-square root of the charge density and is shown in the middle panel of Figure 14 for nominal ionospheric conditions.

The presence of a minimum in the phase speed at approximately 300km altitude in the F-region of the ionosphere indicates that electromagnetic waves may propagate horizontally near the minimum in the Alfven speed. This region is termed the "ionospheric wave guide" or "duct."

Many investigators (e.g. Greifinger and Greifinger, 1968, 1973) have carried out theoretical analyses of this situation and, indeed, there are two electromagnetic wave modes that can propagate in the wave-guide. The wave amplitudes of the two modes are shown in the left panel of Figure 14. The dominant mode, labeled δEy, is the mode that propagates horizontally along the duct. The second mode, labeled δEx, is constrained to propagate along the (vertical) magnetic field direction. Analysis shows that the two wave fields are coupled by currents that depend upon the Hall conductivity. Observations that provide evidence of ducting of naturally occurring electromagnetic waves have been made for many years and will be described below.

As the right panel shows, the Hall conductivity is largest at the bottom of the wave-guide. Although the maximum normally lies between 100km and 125km the conductivity is significant over an interval from 80km to 150km. This is the key to our proposal. We hope to heat the ionosphere in the region where the Hall conductivity is large so that the ambient electric fields

can drive currents large enough to radiate electromagnetic energy into the duct, coupling the locally stimulated wave to the propagating mode.

While the theory of propagation in the ionospheric wave-guide is well established, some of the predictions of the formulations have never been verified. Among these is the presence of a low-frequency duct cut-off similar to the cut-off characteristics of electromagnetic wave-guides. A second prediction of the theory is an attenuation rate that is expected to be on the order of a few dB per 1000 km. However, the predictions vary and have never been measured.
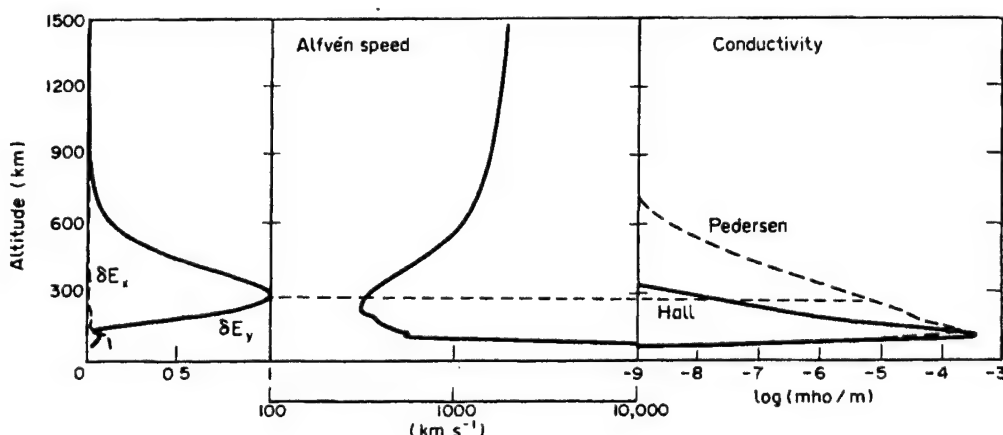
Figure 14. This Plot Shows the Variation of Ionospheric and Wave Properties with Altitude that are Important in the Study of Ducted Electromagnetic Waves. The Left Panel Shows the Electric Field Perturbations of the Waves; the Center Panel Shows the Variation of Alfven Speed of the Waves; the Right Panel Shows the Variation of Hall and Pedersen Conductivities. This Diagram is Taken from Fujita (1978) and Represents Nominal Daytime Conditions.

2.2.1.2 Ducting of natural ULF emissions

For several decades electromagnetic waves in the Ultra-Low Frequency (ULF) band (dc to 3hz) have been detected by magnetometers at the earth's surface (see von Stetten, 1999). The waves have been identified as electromagnetic ion-cyclotron waves that are the result of instabilities in the distant equatorial magnetosphere. Principally generated in the equatorial regions near L=4 on the afternoon side, these pulsations propagate along the magnetic field to the ionosphere. Once incident on the ionosphere they have been shown to be ducted to regions far from the source field line.

When the polarization state of the various classes of Pc1 signals are analyzed a mixture of right-hand and left-hand polarization is observed. Since the left-hand mode cannot propagate in the ionospheric wave-guide while the right-hand polarized wave can, the presence of right-hand signals indicates the pulsation has traveled to the observation point via the ionospheric wave-guide. Also, the attenuation rate of waves propagating along the duct has not been measured.

2.3 Methods, Assumptions and Procedures

The experiment was set up so that the HAARP heater would heat the D-region of the ionosphere with a carrier frequency of 3.3 MHz while modulating the amplitude of the radiation as a sine wave at frequencies in the ULF range of 0.1-1.2 Hz.

For the experiment we chose four different beam modulation frequencies: 0.3, 0.5, 0.7, and 0.9 Hz, and we heated in the X-mode at each modulation frequency for 15 minutes. Below is the time log of our experiment:

14

Table 4. Experiment Log

Time (UTC)	Frequency (Hz)
02:30:00	0.3
02:44:30	**off**
02:45:00	0.5
02:59:30	**off**
03:00:00	0.7
03:14:30	**off**
03:15:00	0.9
03:29:30	**off**

2.4 Results and Discussion

Using synchronous detection techniques we scanned the induction magnetometer data from College and Kaktovic, Alaska during the periods that the HAARP heater was operating in the ULF modulation modes we requested. We did not detect signals above our threshold of 2 pT.

2.5 Conclusions

Although we have evidence that the ionospheric duct was "open" (natural ULF signals were observed during the experimental period) we did not observe any signals associated with the HAARP heating above our instrument threshold. We believe that this may be due to the configuration of currents that flow in the heated region. If the currents are not linear but rather coruscated then it may be that their effective dipole moment is small yielding small radiated field amplitudes. It is our intention to continue these experiments in the hope that we may find the ambient conditions that will allow for successful stimulation of ULF waves.

3. ELEMENT 3: IONOSPHERIC MODELING

3.1 Summary
This element of the HAARP project developed a simulation model for the plasma physical and electromagnetic effects of localized ionospheric heating with the purpose of predicting outcomes of heating experiments and to guide the design of new experiments. Modeled properties are densities, velocities, and temperature of electrons and ions as well as electric and magnetic perturbations up to a frequency of about 1000 Hz.

The development has been conducted in three steps:
- An initial two-dimensional model is completed including a verification of results through comparison with various test cases.
- A pre-existing three-dimensional simulation model has been tailored and updated in terms of ionospheric physics and transport parameters.
- The three-dimensional model has been modified for parallel supercomputers with excellent parallel performance.

3.2 Introduction
Subject and Purpose. The goal of this project was the development of a numerical simulation model for ionospheric heating experiments. A simulation of ionospheric heating and its plasma physical and electromagnetic effects can be of large importance to understand unresolved physical problems of ionospheric modifications and to guide heating experiments.

Scope and Plan. The simulation must include the relevant ionospheric physics which in particular includes: (1) Ionization and recombination; (2) ion-neutral friction; (3) a form of Ohm's law which includes Hall physics and the electron pressure effects; and (4) equations for electron and ion energies including heat conduction.

Such a model is able to realize physics down to the ion inertia scale of about 1 km (at the relevant ionospheric heights) and temporal scales up to about 1000 Hz. Considering the geometry of the heating processes a three-dimensional model is required for many applications.

The simulation model makes is possible to study the ionospheric modifications for instance due to changes of the ionospheric conductances. The generation of hydro-magnetic plasma waves as a result of the heating and consequences for corresponding observations can be analyzed and predicted.

The work proceeded by
- extending an existing two-dimensional model to HAARP specific ionospheric parameters.
- including ionospheric transport parameters and physics in an existing three-dimensional simulation code.
- parallelization of the three-dimensional simulation code for fast performance on parallel supercomputers.

3.3 Methods, Assumptions and Procedures
The simulation model is aimed at meso-scale ionospheric physics (1 km to few 100 km). This is accomplished by using a three-fluid approximation that covers electron, ion, and neutral dynamics. For each species the simulation model integrates the continuity equation, the momentum equation, and the energy equation. To facilitate the desired scales electron inertial

effects are neglected (20 m scale). Otherwise the complete fluid moments are solved in a time-dependent fashion.

The continuity equations contain effects of ionization and recombination in a parameterized form. The momentum equations consider plasma neutral friction, and Ohm's law includes electron pressure gradients and the Hall term. Finally the energy equations include heat conduction and a defined localized heat source in addition to heating by precipitation and frictional (Joule heating) causes.

The ionization rate, the recombination frequency, and the electron heating rate associated with ionization are parameterized by using input from kinetic ionospheric transport computation. The electron heat conduction coefficient and the effective electron-neutral, ion-neutral, and electron-ion collision frequencies are from the National Center for Atmospheric Research (NCAR) thermosphere ionosphere mesosphere electrodynamics general circulation model (TIME-GCM).

The model is based on prior models that we ran for MHD cases and two fluid systems. It uses a Dufort-Frankel integration scheme which is of sufficient accuracy and sufficiently fast to treat the described problem in three-dimensions. The original models have been developed for vector supercomputers and the new model should be parallelized to allow for sufficiently fast performance.

The simulation region extends from 90 km (lower E-region) to 1100 km altitude with the main magnetic field in the vertical direction. The neutral fluid is initially in hydrostatic equilibrium with a temperature T_n and density n_n chosen for solar minimum and solar maximum conditions from the Mass Spectrometer Incoherent Scatter (MSIS) model.

Different from global thermospheric simulation models all physics which plays a role on the considered spatial and temporal scales must be included in the simulation model. This in particular applies to the ion inertia term with the result that typical fluid plasma waves such as Alfven, whistler, fast and slow modes are included in our model. This allows for the propagation of guided ionospheric waves as well as for the formation of field-aligned currents through Alfven waves.

HAARP specific parameters have first been included in an existing two-dimensional simulation code for testing purposes. In the second phase a three-dimensional simulation code was modified to add relevant ionospheric physics and transport parameters. This code has then been parallelized for fast performance on parallel supercomputers.

The parallelization uses message passing (MPI) which has the advantage of portability between different computer systems. The parallelization is applied so that almost the entire code (most of the subroutines) is executed in parallel rather than using parallelization of smaller blocks only. Thus, all time consuming portions of the computation such as the integration routines are executed completely in parallel.

The method uses a one-dimensional domain decomposition, i.e., the total simulation domain is sliced in n subdomains according to the number of processors. This has the advantage that boundary conditions and message passing for gard cells (at the processor boundaries of the subdomains) are significantly easier to formulate. The method generates a bit more overhead in terms of inter-processor communication and we needed to verify that this approach is still very efficient for large numbers of processors (i.e., thin slices with a large fraction of communication to computation time).

17

3.4 Results and Discussion

During the first phase of this project a two-dimensional model has been completed using HAARP specific ionospheric transport parameters. This model served as a test case for the actual three-dimensional model. The model for various applications with the purpose of verifying the simulation techniques and to identify new physical insight of meso-scale dynamics.
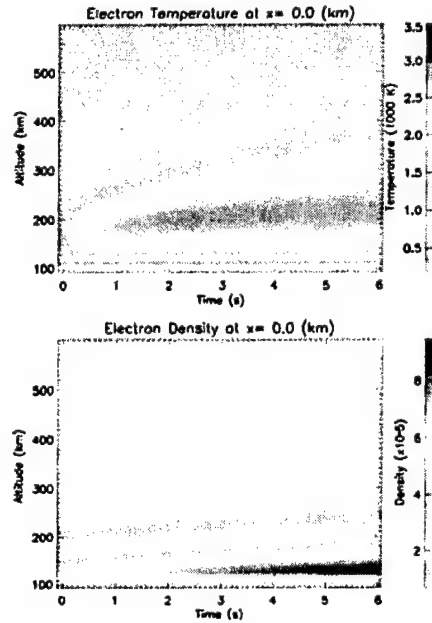
Figure 15. Electron Temperature and Density as a Result of 1keV Electron Precipitation.
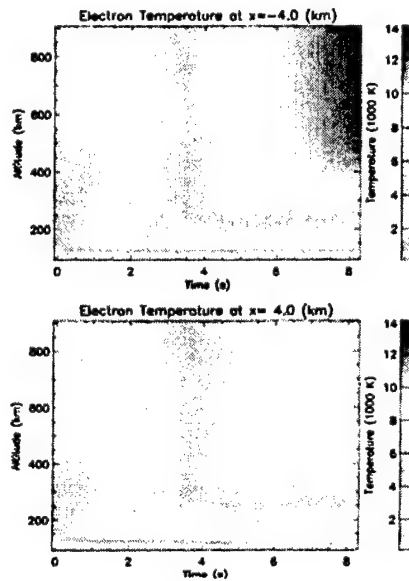
Figure 16. Evolution of the Electron Temperature in a Strong Upward (top) and Downward (bottom) Field-aligned Current Layer.

18

- Electron heating by precipitation and field-aligned currents: This work simulates a well-documented event (EISCAT, Lanchester et al., 2001; Zhu et al., 2001) of a discrete auroral arc and the associated ionization and heating. This event is characterized by a highly interesting sequence of electron density, electron temperature, and ion temperature evolution. The 2-D simulation model demonstrated that the sequence of events is nicely consistent with a combination of precipitation and the passage of a strong field-aligned current layer through the field of view of the EISCAT radars. Figure 15 shows an example of the electron density and temperature evolution as caused by precipitation.

- A similar application is the formation of tall red auroral rays. The formation of tall red rays in the ionosphere has been a longstanding unresolved problem of auroral physics. These rays are pencil-like structures that can extend from 150 km at their base to as high as 600 km. At these heights it is very difficult to deposit sufficient power in order to account for the luminosity of tall rays. The two-dimensional simulation examines ohmic heating by collisional processes in strong field-aligned current sheets to account for visible tall rays. Figure 16 shows the evolution of the electron temperature profile which is quite different from heating due to electron precipitation.

We find that a filamentary current density of about 600 micro A/m^2 over about ten seconds can pump sufficient energy into the ambient oxygen atoms to produce visible auroral red rays. The ohmic heating leads to an electron temperature in excess of 10,000K in the upper F-region. The following figure shows the source and loss terms for the electron temperature (Figure 17), the temperature distribution, and the brightness of the resulting O(^{1}D) emission (Figure 18). This work is highly relevant for the observed redline emissions from auroral heating experiments.

Sources and Losses for Te (eV/s)
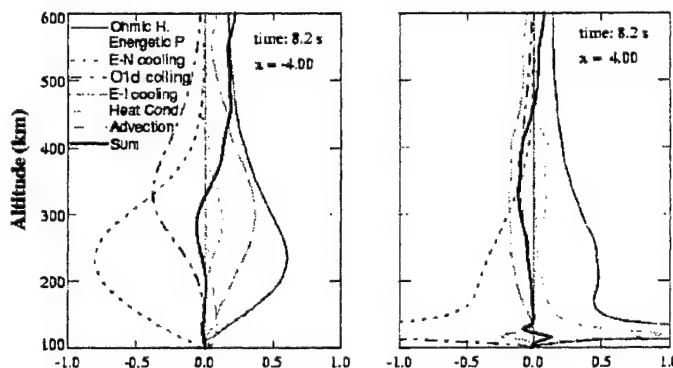
Figure 17. Source and Loss Terms for the Electron Temperature as a Function of Altitude.
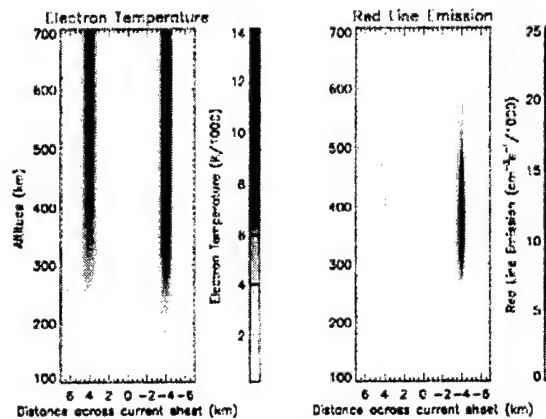
Figure 18. Grayscale Plots of Electron Temperature and Red Line Emission (in kRayleighs).

- Electrodynamic properties of the model have been tested by studying the formation and the evolution of field-aligned current in the ionosphere. This includes the closure of these currents through Pederson currents and the associated Hall currents. Current layers are generated by Alfven wave packets that are launched from the top boundary (magnetosphere). It is noteworthy that the model shows strong density modifications because field-aligned currents are carried by electrons and Pederson currents are carried by ions so that for instance a convergent or divergent ion flow generates strong density enhancements or depletions.
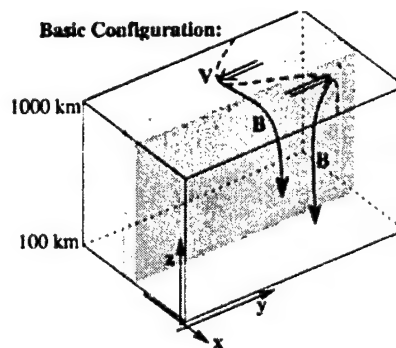
Figure 19. Basic Configuration for the Three-Dimensional Model of Current Sheet Evolution.

The second phase of the project required incorporating self-consistent ionospheric physics and transport parameters into a three-dimensional model. These include the various collision frequencies, electron heat conduction, ionization, and recombination. There were various tests conducted during this implementation similar to the two-dimensional applications. Specifically, we examined wave propagation, generation of field-aligned currents, and effects related to Joule and other heating mechanisms. A noteworthy result from these applications is the generation of vortex flows and auroral structure. The basic configuration for these cases is sketched in Figure 19. A field-aligned current layer is generated by a shearing plasma motion at the top boundary

20

(magnetosphere). To model auroral dynamics the model assumed a localized parallel electric field that is switched on at a critical current density. Without this localized parallel electric field the system only forms a simple current layer as in the two-dimensional cases. The parallel electric field serves as a source for Alfven waves which initiate a three-dimensional vortex motion. Figure 20 shows the result of this motion in terms of the field-aligned current at a fixed altitude in the ionosphere.
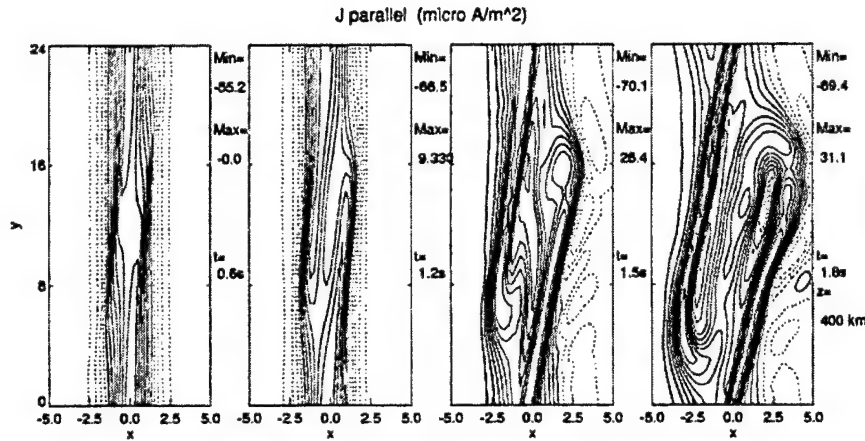
Figure 20. Snapshots of the Field-aligned Current Geometry in the Three-dimensional Simulation.
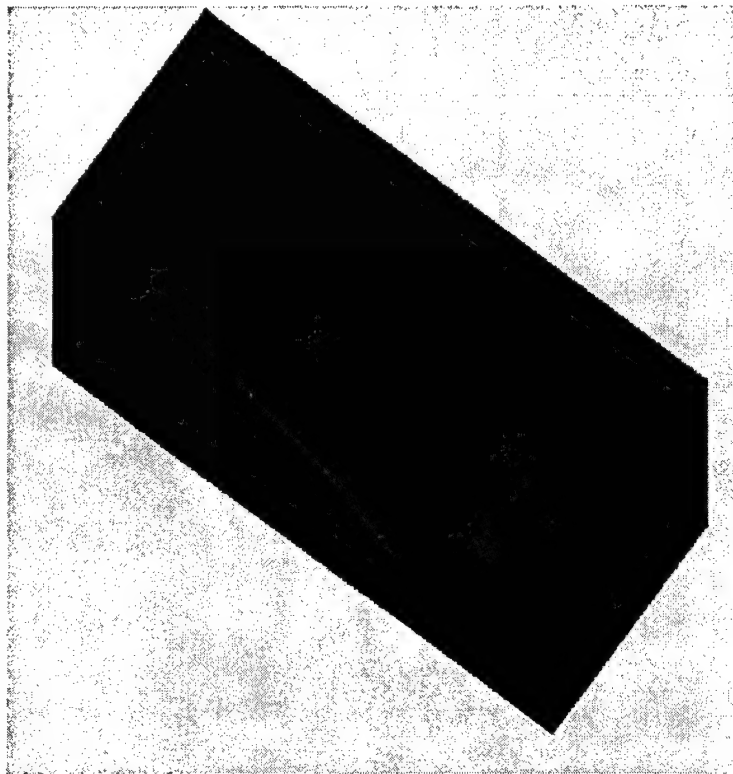
Figure 21. Image of Auroral Emissions Generated from a Three-dimensional Simulation Run.

21

By integrating the parallel electric field along magnetic field lines it is possible to determine the energy of the precipitating particle. With this energy map and auroral excitation profiles we were able to generate a view of the resulting auroral structure which is shown in Figure 21. The overall structure is highly reminiscent to actual aurora and to our knowledge this is the first model of a simulated discrete auroral structure.

To run the three-dimensional model on modern parallel supercomputers with distributed memory it was necessary to parallelize the 3D simulation code. The parallelization was conducted using the message passing instruction set (MPI). The simulation method is highly suitable for a parallelization because the integration scheme only requires next neighbor communication for the individual grid cells.
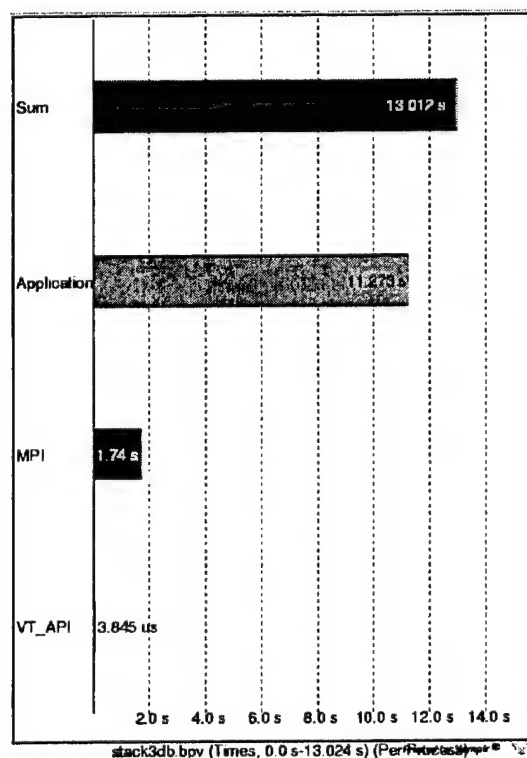
Figure 22. Chart of Total, Computation, and Communication (MPI) Time for the Parallel Code (8 Processor and 7 Grid Cells Across Subdomains).

To achieve a highly parallelized code many of the individual subroutines are carried out completely in parallel. The total simulation domain is sliced in n subdomains each of which is computed by a separate processor. The major advantage of using slices along one direction vs. slicing the total domain in two or three directions is a much simpler implementation of the message passing instructions for the grid cells of each domain. The trade-off is a somewhat larger amount of information that has to be passed between subdomains. The crucial question for this approach is whether a high parallel efficiency could be maintained for very thin slices in terms of the number of grid cells across each subdomain. We found that that this approach turned out to be highly efficient even for cases with only 5 grid cells across individual subdomains. In this case the message passing overhead was acceptable (50 to 100%) for up to 100 processors. For the case of 8 processors with 7 gridpoints across the figure to the right demonstrate a very high efficiency (85%) or rather small amount of time consumed by the inter-processor-

22

communication (MPI). We expect that this should be further improved if input and output is conducted in parallel with a new implementation of MPI.

3.5 Conclusions

1. We have expanded a two-dimensional meso-scale simulation model to include ionospheric physics and transport parameters relevant for the HAARP facility. The new simulation code has been applied to a variety of ionospheric phenomena with focus on the formation and evolution of field-aligned currents, Alfven wave propagation, electron and ion heating, and ionization through particle precipitation. The results and applications have provided new insight into the current closure and resulting density modification in the ionosphere, the mechanism for the formation of tall red auroral rays, and the source and loss mechanisms of electron energization in field-aligned currents.

2. Based on the two-dimensional results we have implemented ionospheric transport into a three-dimensional simulation code. Applications and test of this code were similar to the 2-D applications. In addition three-dimensional dynamics was studied with application to the formation of auroral arcs. As a major result the three-dimensional dynamics produced the first images of auroral structure produced by a simulation model.

3. The three-dimensional simulation code has been parallelized using message passing (MPI) for parallel supercomputers with distributed memory. The resulting parallel code is very efficient even for large number of processors.

3.6 All Previous and Related Contracts and Previously Produced Publications or Articles

Otto, A. and H. Zhu, Fluid Plasma Simulation of Coupled Systems: Ionosphere and Magnetosphere, in Space Plasma Simulation, (Lecture Notes in Physics), J. Buchner, C.T. Dum, M. Scholer, (eds.), pp.193, Springer Verlag, Berlin Heidelberg, Germany, 2003.

Otto, A., D. Lummerzheim, H. Zhu, O. Lie-Svendsen, M.H. Rees, and B.S. Lanchester, Excitation of Tall Auroral Rays by Ohmic Heating in Field-Aligned Current Filaments at F Region Heights, *Geophys. Res.,* **108**, (A4), 8017, 2003.

4. ELEMENT 4: SUPERDARN OPERATIONS

4.1 Summary

Construction of the Kodiak SuperDARN radar was completed in January 2000 and the radar has operated continuously since that time. Each HAARP campaign since January 2000 has been supported with observations from the site. Electric field measurements have been available continuously and special operating modes have been implemented for specific experiments. Special operating modes were executed on nine days during this reporting period for a total of 39 hours of radar operation. The objective of the special operating modes was to examine the formation of ionospheric irregularities within the heated volume and to examine the relationship of the irregularities to other observations such as the generation of Stimulated Electromagnetic Emissions (SEE).

4.2 Introduction

The Kodiak SuperDARN radar is an HF radar that was built as part of the SuperDARN radar network. SuperDARN, the Super Dual Auroral Radar Network, consists of eight HF radars in the northern hemisphere and six radars in the southern hemisphere that were built to observe the signature of magnetospheric convection in the ionosphere. Radio signals are reflected from irregularities of the ionospheric plasma, that are generated naturally by plasma instabilities induced when an electric field is applied across plasma density gradients. At high altitudes, these plasma irregularities move with the bulk velocity of the plasma and, hence, the radio reflections can be used to trace the motions of the bulk plasma. The bulk motion follows the magnetospheric convection pattern and, by combining data from all the radars in the network, the convection pattern can be mapped and monitored as it changes in response to changing interplanetary conditions.

In addition to the global-scale convection pattern, the data are of sufficient resolution to determine the local electric field above the HAARP site. This electric field data can be used in conjunction with other observations and computer models to aid in understanding the generation of ELF from the heated volume.

Ionospheric heaters, such as HAARP, also induce plasma instabilities that produce irregularities from which radio signals scatter. While the instabilities are not the same ones that operate naturally, the resulting irregularities can be detected by an HF radar. Hence, the Kodiak SuperDARN radar acts as an excellent diagnostic of the ionospheric heating produced by HAARP.

4.3 Methods, Assumptions and Procedures

The Kodiak SuperDARN is a phased array radar operating in the HF frequency band (8 MHz to 20 MHz). The radar is steered electronically in 16 fixed azimuths separated by about 3.25° covering an azimuth sector of about 52° that is centered along an azimuth of 30° east of true north. The radar transmits a beam that is narrow in azimuth, about 3°, and broad in elevation angle; about 15° half power beam width. The peak elevation angle of the beam is in the range of about 10° to 20° above the horizon depending on frequency. Because the signal is in the HF band, the signals are subject to refraction in the ionosphere and long distance propagation is possible. It is not uncommon for the radar to observe ionospheric scatter at ranges of more than 3000 km. The radar transmits short pulses and samples each beam direction into 75 range bins. The size of the range bins depends on the transmitted pulse length and usually is in the range

from 15 km to 45 km. The radar dwells in each beam direction for a period of time, usually in the range from 1 second to 7 seconds, and integrates returns over the period. With these dwell times, the time to complete a sweep of all sixteen beams ranges from about 20 seconds to 2 minutes.

The signals are scattered from electron-density irregularities in the ionosphere; mostly from the F-region ionosphere. The scattering process is Bragg reflection, so the radar is sensitive to irregularities with spacing equal to one half of the radar wavelength. Hence, the radar senses the presence of decameter scale irregularities. Such irregularities are produced naturally through the gradient drift instability and are produced in the artificially heated volume through other instabilities. The scattering is a coherent process, so the scattering cross section is quite large and the radar needs to transmit only low power.

Special operating modes created for HAARP observations included high-range resolution, reduced scans, and repeated beams. The ionospheric volume above HAARP sits at about 650 km to 700 km range from Kodiak at an azimuth of about 30°. Scatter from the heated volume typically appears in the central eight radar beams. By scanning over only those central eight beams, the time to complete a scan is reduced and higher time resolution is achieved. The other way in which we have achieved high time resolution is to interleave a single beam between each beam of a scan. That is, the beam sequence would be beam 8, beam 4, beam 8, beam 5, beam 8, beam 6, beam 8, beam 7, etc. If the integration time for each beam is3 seconds, then this mode would provide time resolution over the HAARP site of about 6 seconds.

4.4 Results and Discussion

Radar scatter from the artificial irregularities has been observed during each of the scheduled experiments. Figure 23 shows a time series of the scatter observed on 7 August 2000. These data were taken during the HAARP summer school campaign in support of the experiment to generate SEE. The heater was cycled on and off and the irregularities appear and disappear with the heater cycle.
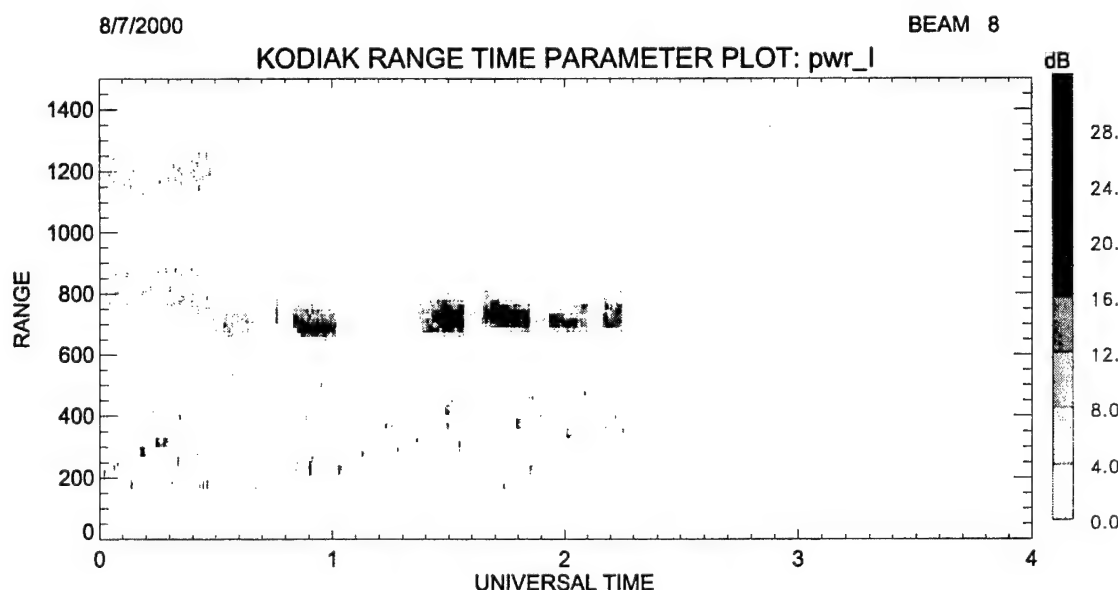
Figure 23. Power vs. Range of Radar Scatter from 7 August 2000 Between 0000 and 0400 UT.

At the beginning of this interval, there was significant ionospheric absorption and no SEE were observed, and no ionospheric irregularities were observed. As the figure illustrates, the absorption abated as the experiment continued and irregularities were observed. SEE were observed at about the same time that the irregularities appeared.

Figure 24 shows some of the same data superimposed on a map of Alaska to illustrate the spatial extent of the scatter above the HAARP facility. Scatter is observed in 6 beams and in about 8 of the 15-km range gates covering a range of about 120 km. The region appears larger in azimuthal extent than in range extent because of the finite beam width of the antenna beam pattern. The observation is the convolution of the beam pattern with the area of irregularities.
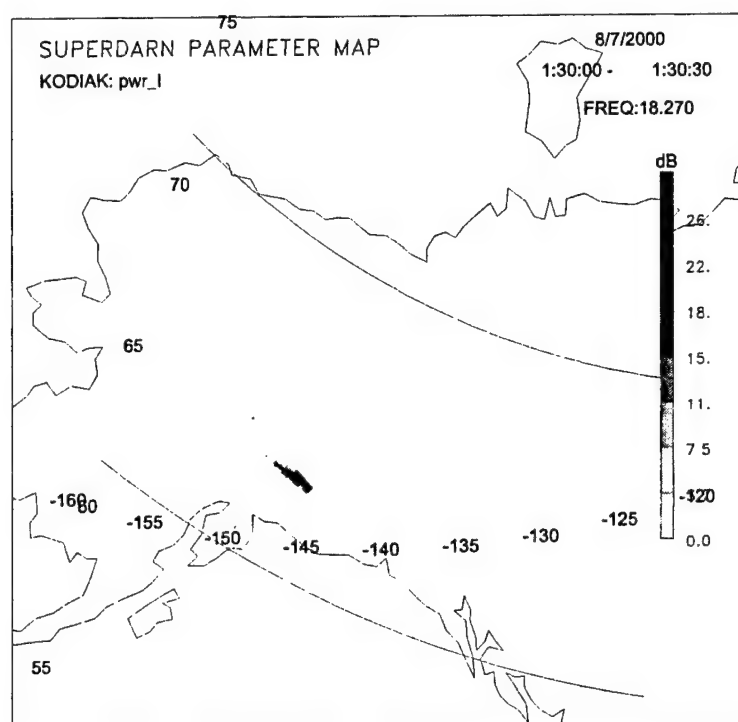
Figure 24. Geographic Projection of Scattered Power at 0130 UT on 7 August 2000.

The following paragraphs present an example of the experiments carried out under the contract. During the Polar Aeronomy and Radio Science (PARS) summer school in 2002, a 'plasma line' experiment was performed along with Frank Djuth and Mike Sulzer. This experiment used the HAARP ionospheric heater in a mode that was ideal for simultaneous field-aligned irregularity (FIA) observations. HAARP transmitted O-mode at a frequency near FoF2 at full power. During the experiment, there was a 25 minute sub-experiment during which the heater was operated on a cycle of 5 seconds on, 25 seconds off. The Kodiak SuperDARN radar was used to observe the formation and decay of FAI during the sub-experiment.

The radar did not scan during the experiment, but rather continuously observed directly over the HAARP site (beam 8 of the radar). The range resolution of the radar was set at 15 km. The integration time of the radar was set at 1 second. Figure 25 shows range-time-intensity (RTI) plot for 10 heater on-off cycles.

26
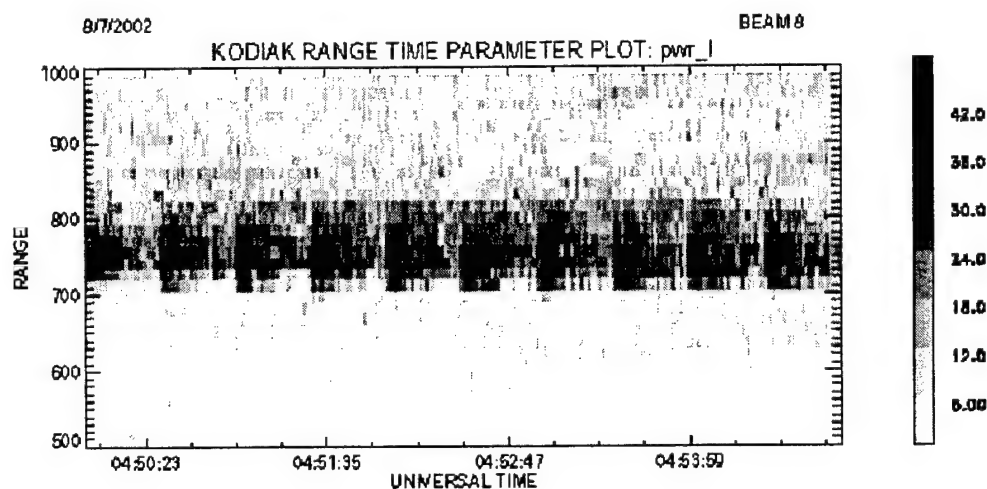
Figure 25. RTI Plot for Showing the Signal-to-Noise Ratio (SNR) from 04:50 to 04:55 UT on 7 August 2002. The Periods of Intense Return SNR Correspond to the HAARP Heater-on Times, Indicating the Formation of FAI.

This figure illustrates that there is a FAI formation time and decay time that may be extracted from the radar data. When the time series of one radar range gate is observed, the data is too 'noisy' for good curve fitting. Averaging over range alleviates this problem. Figure 26 shows a time series of the same data in Figure 25. This data is averaged over range 705 km to 795 km corresponding to the heated region of the ionosphere.
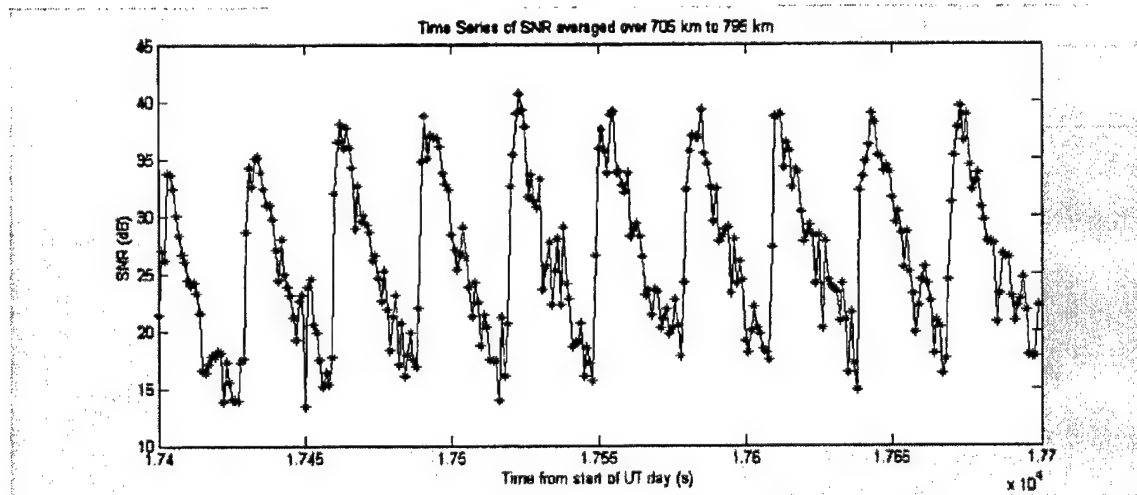
Figure 26. Time Series Plot of SNR Averaged Over 705 km to 795 km.

To get information on the formation time of the FAI can the HF radar data from each heater on-off cycle is isolated. A curve of the form $1 - e^{\frac{-t}{\tau}}$ is optimally fitted to the rising edge of the FAI data using a non-linear least-squares fit. This is illustrated in Figure 27. The data shown correspond to the fifth heater on-off cycle shown in Figures 25 and 26.

27
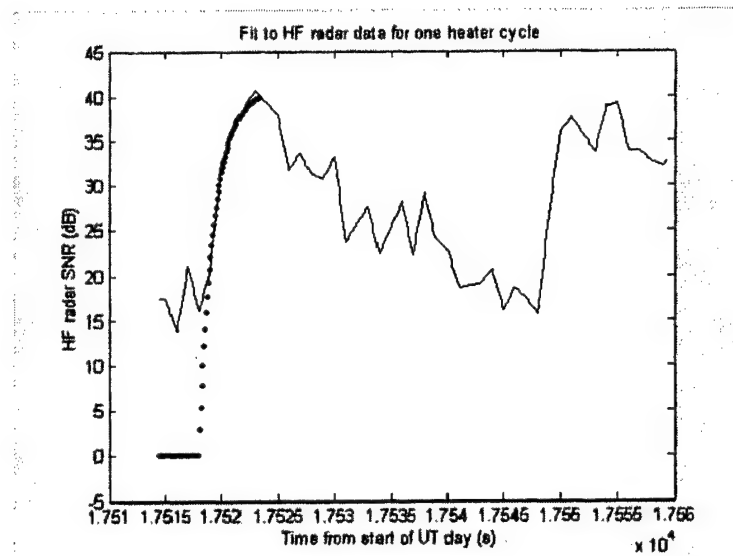
Figure 27. Optimal Non-linear Least-squares Fit an HF Radar Observation of a HAARP Heater Cycle. This Fit Corresponds to the Formation of FAI.

The formation time of the FAI can be determined from the non-linear least-squares fit. In the case in Figure 27, the FAI formation time constant, τ, is 0.7 seconds. When the FAI formation time constant is calculated for each heater on-off cycle, a trend in the FAI formation time constants can be seen over the time of the experiment. The FAI formation time constant for each of the 50 heater on-off cycles in the 25 minute sub-experiment is shown in Figure 28.
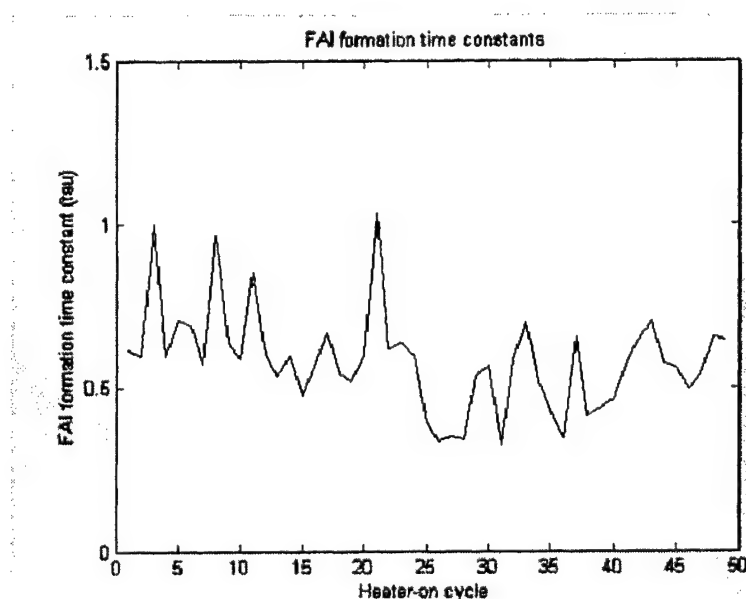
Figure 28. FAI Formation Time Constants for Each of the 50 Heater On-Off Cycles.

This plot shows that there is some change in the FAI formation time constants over time. More data over a longer time would be ideal for characterizing this trend. Future experiments of this type will be necessary to determine the geophysical conditions that affect the formation time.

28

4.5 Conclusions

It can be concluded that the Kodiak SuperDARN radar is capable of observing scatter from ionospheric irregularities generated within the volume heated by the HAARP facility. The irregularities appear to be generated whenever ionospheric conditions allow the heater signal to reach the F-region ionosphere. The scattering cross section of the heater-induced irregularities is generally large, allowing for short integration times. In recent experiments, the radar integration time has been as low as 1-second per beam and produced adequate signal-to-noise ratio to observe the heater-induced irregularities. The induced irregularities appear to have a finite decay time and do not disappear until some period of time after the heater is turned off. The decay time appears to be lengthened when there is a significant ambient electric field. It is also possible to determine the formation time for irregularities as illustrated in the preceding section. Planned improvements to the radar hardware and software will allow improved spatial and temporal resolution.

4.6 Recommendations

It is recommended that experiments be continued using the Kodiak radar. Specific experiments to determine the time required for irregularity generation and the heater power required should be carried out.

5. ELEMENT 5: HAARP EDUCATION OUTREACH PROGRAM

5.1 Summary

The HAARP Education Outreach program provides scientific education (about HAARP specifically and physical science in general) to members of the local Copper Valley community. This is done through direct involvement in local schools in the Copper River School District (CRSD) and the Prince William Sound Community College (PWSCC), as well as public lectures and workshops, and intern and student research programs. The program has also facilitated cooperation and coordination between other organizations interested in promoting science education in the region, such as the National Park Service (Wrangell- St. Elias National Park). The HAARP Education Outreach Program has been active for over five years and in that time has become an integral part of science education in the Copper Valley for residents of all ages. We have found that by being a "good neighbor" and helping meet the educational needs in the region, we have also begun to gain the public's trust concerning the HAARP program itself. In addition the program has actively been involved in helping to create the Wrangell Institute for Science and the Environment (WISE), which is a non-profit organization with a specific charter of enhancing scientific research and education in the region.

5.2 Introduction

The chief objectives of the HAARP Science Outreach Program are to: 1) enhance scientific knowledge and understanding; 2) provide science education and training opportunities in the Copper Valley for students and the public; 3) educate local residents about the HAARP Research Program; and 4) facilitate the direct involvement of Alaskan students and teachers and also the local Copper Valley community in HAARP research campaigns and in the use of HAARP on-line data.

5.3 Methods, Assumptions and Procedures

These objectives are accomplished through a variety of education outreach programs in the CRSD schools, the local community and also at PWSCC and UAF. These are done in cooperation with the newly formed Wrangell Institute for Science and the Environment (WISE), Wrangell St. Elias National Park and PWSCC in Glennallen.

The school programs include: direct classroom involvement, development of science kits for use in the schools, workshops with K-12 teachers and encouraging appropriate high school research collaborations between HAARP researchers and interested students primarily through the HAARP High School Summer Internship Program. We also have an internship program at UAF, which is cooperatively connected with the Geophysical Institute Summer Internship Program. The education programs for the larger community include physics demonstrations (now called "Bush Physics in the 21st Century") at the annual HAARP Open House, public lectures given by HAARP researchers and other scientists who do research in the region, and our participation in, and support of, other community-based science education programs.

We work closely with teachers in the schools, adapting to their needs and the particular scientific topic they are covering at the time. In the higher grades and larger schools, more coordination and planning are necessary because the curriculum requirements are more stringent. Because of time and necessary logistic constraints, the outreach visits are episodic, occurring roughly four times a year. Even though the in-class time per year is not large, our experience suggests that a long term, multi-year connection enhances learning by the students. We also try

30

to coordinate with HAARP campaigns to utilize the availability of top scientists for public lectures. Also it is very important to respond when regional needs arise: such as, following the 2002 Denali Fault Earthquake.

Education Outreach trips to the Copper Valley are usually 1-3 days and involve D. Solie and since spring 2003 have involved a UAF Alaska Native Science and Engineering student.

UAF summer interns work primarily at the Geophysical Institute and those from Glennallen work at the HAARP site in Gakona or at a partner institution for a portion of their internship.

5.4 Results and Discussion

The following is an abbreviated listing of the Education Outreach activity from 29 July 1998 to 30 January 2001 and a full listing from 31 January 2001 to Summer 2003.

First 18 Months:

Participation in annual HAARP Open House in Gakona "Mr. Wizard" science demonstrations (1999 & 2000)

Sponsored HAARP Popular Lecture Series in cooperation with Prince William Sound Community College (Spring 2000, Fall 2000)

Regular visits to public schools in the Copper Valley to give science presentations and involvement in Copper Valley schools including Chistochina School, Gakona School and Glennallen High School (Fall 1999, Spring 2001)

Presented a science workshop for public school teachers as part of a Copper Valley School District Teacher training in-service (November 1999)

Involvement in developing a Science Center in the Copper Valley (Spring 2000–present)

Facilitation of Glennallen High School student/HAARP researcher research project (Fall 2000-present)

Instigation of High School Student Summer Intern Program at HAARP (summer employment for a high school student in the Copper Valley at the HAARP site) (Summer 1999, Summer 2000)

Instigation of a HAARP University Student Intern Program at UAF (Summer 2000)

Final 30 Months:

Spring 2001

HAARP Popular Lecture Series on SPRITES (in cooperation w/ PWSCC)

Very Low Frequency Research in Antarctica and Colorado

Rob Moore

2-3 March 2001
Lecture and short course on Mt. Wrangell (PWSCC); hands-on science presentation in Chistochina School and Gakona School
Carl Benson, Daniel Solie

25 & 26 August 2001
"Mister Wizard" physics demonstration show at HAARP Open House
Daniel Solie

22-25 October 2001
Present science demonstrations in Chistochina, Copper Center & Gakona School; WISE Board meeting
Daniel Solie

3-5 December 2001
Science demonstrations in area schools: (Kenny Lake High School, Chistochina and Gakona)
Daniel Solie

22 –25 January 2002
Science demonstrations in Glennallen High School science classes and Copper Center school; met with Copper Valley School District Superintendent and Principals of all area schools to outline the HAARP Education Outreach Program for schools
Daniel Solie

1-2 & 8-9 March 2002
HAARP/PWSCC short course for teachers "Hands-on Physics: Waves in Sound and Light, on Earth and in Space" presented in Glennallen at PWSCC
Daniel Solie, John Peterson

9-11 April 2002
Gakona School tour of HAARP site; science presentation on basic mechanics to Chistochina School, attend WISE board of directors meeting; science presentation on solar system to Copper Center School 4-6 grade class
Daniel Solie

10 & 25 April 2002
Arranged tours of HAARP site for area schools (Gakona School, 10 April)
Daniel Solie
and the accelerated math class from Copper Center School (25 April)
Marty Keskinen, Daniel Solie

28 April–1 May 2002
Attended RF Ionospheric Interactions Workshop; presented poster and abstract titled "The Science Education Outreach Program at HAARP"
Daniel Solie

<u>14-16 May 2002</u>

Lecture and demonstrations on electromagnetic waves, Glennallen High School physics class; interviewed HAARP high school intern candidate

Physics lesson on rockets to 4-6-grade class at Copper Center School. Rocket demonstrations at Chistochina School and Gakona School (16 May)

Ed Kennedy, Daniel Solie

Summer 2002

Summer High School Intern Program at HAARP

(Intern: Troy Lawlor)

Ed Fremouw, John Rasmussen, (Daniel Solie)

Summer 2002

HAARP- UAF Summer Intern Program

(Intern: Eric Adamson)

Antonius Otto, (Daniel Solie)

<u>21-22 November 2002</u>

Lectures/slides and demonstrations on the 3 Nov. 2002 Denali Fault Earthquake (mag. 7.9) Gakona (pop. 239) >30 attend, Glennallen (pop. 517) >60 attend, Glennallen High School >200 attend, Salana (pop. 107) >100 attend

Patty Craw (Alaska State Geological Survey), Suzanne McCarthy (PWSCC), Daniel Solie

<u>21-22 February 2003</u>

First WISE Lecture/Open House: Seismology, slideshow and demonstrations on the 3 Nov. 2002 Denali Fault Earthquake (mag. 7.9) Wrangell-St. Elias National Park Headquarters (68 attend)

Hillary Fletcher (AIEC GI-UAF), Suzanne McCarthy (PWSCC), Daniel Solie

<u>9-11 April 2003</u>

Joint Education Outreach trip: HAARP Ed Outreach, PICES (San Diego State) and Geophysical Institute

Science lessons and hands-on demonstrations to Copper Valley schools

Daniel Solie, Theresa Sanchez and Glen Kinsoshita (San Diego State), Matt Gho (UAF ANSEP/PICES student)

Presentations were made in all public schools in the CRSD

<u>April 2003</u>

Geology presentation at PWSCC

James Battis

Summer 2003

(Note: continuation of program under PARS2)

2003 Summer High School Intern Program at HAARP

(Interns: Troy Lawlor and Josh Horvath)

Ed Fremouw, Paul Kossey, Ed Kennedy, John Rasmussen, (Daniel Solie)

Summer 2003
(Note: continuation of program under PARS2)
HAARP-UAF Summer Intern Program
(Intern: Jeff Mann)
Antonius Otto

Science Kits & Demonstrations Developed and/or Deployed (as of Fall 2003):

A) Simple Machines: Levers, Pulleys, Potential Energy and Work

B) The Spectrum of Light

C) Waves

D) Resonance in Sound and Buildings

E) Scaling the Solar System

F) AURORA Alive! – Middle School curriculum developed by the Geophysical Institute

G) Radioactivity, Leaky Water Bottles and Exponential Decay

H) Water Rockets!

I) Electricity and Charge

J) Magnets and Motors

K) Seasons of the Earth

L) Optics: Bending Light, Jello Lenses and How to Make A Telescope

M) Measuring the Speed of Sound Three Ways

N) Determining the Speed of an Arrow:
   The Old Way (Basic Physics, a Little Algebra and a Simple Pendulum)
   and The New (Faraday's Law, Fast Electronics & Simple Math) (developed in 2003)

5.5 Conclusions

The Education Outreach Program has been successful in achieving the program goals. While quantitative assessment of the educational gains was beyond the scope of this project, strongly positive responses from CRSD teachers, students and administrators are evidence of the program's success. In addition, teachers from Gakona School and Chistochina School (the two schools closest to the HAARP site and the ones most often visited) reported that students in their schools correctly answered questions on the most recent CAT standardized exam, on material which had only been presented by the HAARP Education Outreach Program. This indicates that even though the in-class time per year is not large, a long term, multi-year connection enhances learning by the students.

The HAARP Education Outreach Program, which has now been active in the region for over five years, is a trusted source of scientific information. A demonstration of this was following the

2002 Denali Fault Earthquake, teachers from schools in the Copper Valley contacted us and requested we come down and explain what happened. As a result we collaborated with a field expert from the Alaska State Geological Survey (P. Craw) who had just returned from the field where she was part of the team that was studying the surface rupture caused by the quake and Suzanne McCarthy (also a geologist) from PWSCC. This outreach trip was I believe, the best thing the HAARP Outreach Program has ever done. The large turn out, and enthusiastic and grateful response of people in the strongly affected areas of Chistochina, Gakona, Salana and Mentasta was humbling and it was a privilege to be part of it. It demonstrated that a timely response to real questions and giving the people some understanding of the "how" behind a natural event was, in itself, healing.

In June 2003, Chris Jonientz-Trisler, Regional Earthquake Program Manager from the Federal Emergency Management Agency (FEMA), Region 10, highlighted our experience and what we learned at a National Disaster Response Conference held in Washington DC. The following is an excerpt from her presentation:

Another outreach team visited the area at the same time the FEMA Earthquake Program Manager was visiting schools 18 days after the earthquake. Their goal was to provide new field information gathered about the event in an attempt to reduce both the mystery of what had happened during the earthquake and the fear factor that remained in the communities. This team was responding to an immediate need for information by residents and found a unique opportunity for the "teachable moment" as Dan Solie describes it.

Post-2002 Denali Earthquake Outreach by Personnel from ADGGS, HAARP/UAF, and PWSCC

A local collaboration team took on the challenge of "a teachable moment" to meet the urgent local need of residents to understand what had just happened to them and what was likely to happen next. The outreach effort was coordinated by Dan Solie, a co-principal investigator with a local public education and outreach program known as the High frequency Active Auroral Research Program (HAARP, funded by the Air Force). He was joined by Patty Craw from Alaska State Division of Geological & Geophysical Surveys (DGGS) and Suzanne McCarthy from Prince William Sound Community College. Patty, a DGGS geologist, had just returned from a week of fieldwork immediately following the M7.9 event along the Denali Fault with a team led by the U.S. Geological Survey. Suzanne is a local educator and administrator with a degree in geology that made observations by fixed wing aircraft shortly after the earthquake. The team scheduled meetings in Glennallen, Gakona and Slana to provide information and reassurance to the residents.

More than one team member observed that the closer a community was to the fault, the more somber the mood of the gathering and the higher per capita attendance at their presentation. People in Slana who were within 15 miles of the fault appeared more traumatized by the event than people farther away in Gakona, 60 miles from the rupture zone, or Glennallen, 80 miles from it. In an attempt to help people deal with their fears, they provided scientific information including a description of the geologic effects of the earthquake, introduced the concept of earthquake recurrence intervals and presented a demonstration of strain build-up and release along a simulated fault using a model borrowed from the Alaska Earthquake Information Center at the University of Alaska Fairbanks. This information suggested that the people living near the fault had most likely seen the worst part of the fault activity during the magnitude 7.9 event. This

was an important issue because they had experienced a magnitude 6.7 along the same fault 11 days previously on 23 October and were continuing to feel aftershock....

...He [Solie] compared the moods of the different communities attending the meetings and how that affected the method of presentation. In Gakona "people were shaken but wanted information" and there were "a few scare stories." In Glennallen 20 miles farther from the rupture, there were "still some people shaken pretty hard, but even more wanted information" and at the high school there was "pure interest." However, in Slana, 15 miles from the rupture, it was "a totally different story. 'Cool stuff' was not the way to present it. They really got shaken there."

Conclusions Related to HAARP/DGGS/PWSCC Outreach Activities

Dan [Solie] says that "by simply giving people the information (about the earthquake), it helped them deal with the whole thing." It was important to have credible information and so it was useful to have geology experts available to speak to the public. The community knew the local education and outreach people and trusted them to bring credible experts and information back to them. Residents wanted information about what had happened and what was likely to happen next.

Summary of General Lessons for Capturing the "Teachable Moment"

We learned lessons about using the "teachable moment" that an earthquake can provide:
  * Use opportunities to find out what are the issues and needs of impacted people
  * Make recommendations to help solve those needs and deal with issues
  * Share issues, needs and recommendations with people who have resources and interest to address them, get local input
  * Short term opportunities - provide information to residents about what happened, what is likely to happen next, what they can do now, and how to do it
  * Longer term opportunities - adapt to new conditions and redesign pre-disaster programs and planned activities to include addressing new or unforeseen issues
  * Collaborate with others and use their expertise in developing credible information
  * Collaborate with locally known outreach programs and people who can provide ease of access and credibility to your own activities
    (email reference: Chris.JonientzTrisler@dhs.gov)

All of the above activities require cooperation with the UAF Physics Department, and close coordination and cooperation with the Glennallen Branch of the Prince William Sound Community College and the Copper Valley School District and also other members of the Glennallen community. In providing science outreach to outlying schools we are filling an important need in the rural schools.

The public lectures, given by HAARP researchers, have two important functions: first they bring interesting science into the community, and second, they educate people on what kind of research is being done at HAARP. Attendance at the public lectures is still growing.

The intern programs, especially the HAARP High Shool Program, has been very successful. In the Copper Valley, our program is, to our knowledge, the only program specifically geared to the scientifically gifted student and thus serves an important role in educating scientists of the future.

In closing, I believe that the above efforts have also helped to improve the standing of HAARP in both the local community and Alaska. It is a privilege to be part of this program and I

want to especially thank Paul Kossey, Ed Kennedy, Jim Battis, John Rasmussen, and Lee Snyder for their help and strong support.

5.6 Recommendations

(These recommendations are currently being implemented under the continuation of HAARP Education Outreach Program now included in PARS2 and funded by ONR)

Involve other UA Education Outreach Programs in the Copper Valley and possibly other areas where HAARP is involved to provide greater leverage and synergy in outreach efforts.

(ANSEP Partner organizations provide internship and scholarship awards on a competitive basis to qualifying ANSEP Native college students majoring in science and engineering. Partner organizations include: Alyeska, BP, Veco, and other oil industry companies, Alaska Native Tribal Health Consortium, Siemens Co., BRIN-UAF (NIH), UAF-Center for Nanotechnology)

Involve UAF and other HAARP related graduate students as well as ANSEP students in education outreach.

Coordinate HAARP Education Outreach with Geophysical Institute Outreach Program (currently doing that with AEIC and the GI Educational Outreach Office)

Coordinate lecture series with the Wrangell Institute for Science and the Environment (WISE) as well as PWSCC

Use Internet and distance delivery technology to more effectively deliver physics presentations to small rural schools in the Copper Valley, especially *"Bush Physics in the 21st Century"* units that are being developed.

Become a Partner Organization with the NSF sponsored Alaska Native Science and Engineering Program (ANSEP) by providing an ANSEP-Internship and scholarship to a qualified Alaskan Native in EE or physics (internship could be w/any institution doing work at HAARP).

5.7 All Previous and Related Contracts and Previously Produced Publications or Articles

UAF: C. Benson, B. Bristow, Vincent Dols, J. Kan, H. Fletcher, R. Hanson, J. Olson, A. Otto, J. Peterson, D. Sentman, R. Smith, D. Solie

HAARP Researchers (non-UAF): J. Battis, E. Fremow, E. Gerken, Ed Kennedy, M. Keskinen, P. Kossey, B. Livingston, M. McCarrick, R. Moore, J. Ostergaard, J. Rasmussen, Lee Snyder, H. Zwi

Other: P. Craw (ADGGS), S. McCarthy (PWSCC), G. Kinsoshita (San Diego State Univ.)

REFERENCES

Fujita, S., Duct Propagation of Hydromagnetic Waves Based on the International Reference Ionospehre Model, *Planet. Space Sci.,* **35**:91-103

Greifinger, C. and P.S. Greifinger, Theory of Hydromagnetic Propagation in the Ionospheric Waveguide, *J. Geophys. Res.,* **73**:7473, 1968.

Greifinger, C. and P.S. Greifinger, Waveguide Propagation of Micropulsations out of the Plane of the Geomagnetic Meridian, *J. Geophys. Res.,* **78**:4611, 1973.

Jonientz-Trisler, Chris, (email reference: Chris.JonientzTrisler@dhs.gov) Regional Earthquake Program Manager from the Federal Emergency Management Agency (FEMA), Region 10, presented at a National Disaster Response Conference held in Washington DC, June 2003, (email communication 5 June 2003)

Lanchester, B.S., D. Lummerzheim, A. Otto, M.H. Rees, K.J.F. Sedgemore-Schulthess, H. Zhu, and I.W. McCrea, Ohmic Heating as Evidence for Strong Field-aligned Currents in Filamentary Aurora, *J. Geophys. Res.,* **106**:1785-1794, 2001.

Solie, Daniel J. and John K. Petersen, University of Alaska, Fairbanks Alaska, "The Science Education Outreach Program at HAARP" Poster presented at the RF Ionospheric Interactions Workshop 28 April – 1 May 2002, Santa Fe, New Mexico

Zhu, H., A. Otto, D. Lummerzheim, M.H. Rees, and B.S. Lanchester, Ionosphere-magnetosphere Simulation of Small-scale Structure and Dynamics, *J. Geophys. Res.,* **105**:1795-1806, 2001.

von Stetten, David, Propagation of Pc 1 Pulsations in the Ionospheric Waveguide: A Review, Master's thesis, University of Alaska Fairbanks, Physics Dept. 1999.

APPENDIX A. Analytic Expressions Used For Modeling ELF Observations

Among the several different approaches to computing electric and magnetic fields at the ground originating from a source buried in the lower ionosphere, the following expressions provided by P.R. Bannister were used to fit the observations described in Section 1.4 above.

- Exact Integral Solutions for horizontal electric dipole (HED) embedded at the base of the ionosphere.
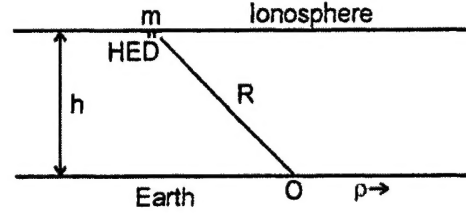
Define the following quantities:

Figure A.1. Geometry of simplified model of the earth-ionosphere cavity, with the Horizontal Electric Dipole (HED) ELF source embedded at the base of the ionosphere of height h above the ground. The observer O is located a distance R from m.

$$u_0^2 = \lambda^2 + \gamma_0^2; \ \gamma_0 = i2\pi / \lambda_{air} \tag{A.1}$$

$$u_e^2 = \lambda^2 + \gamma_e^2; \ \gamma_e = \sqrt{i\omega\mu_0(\sigma_e + i\omega\varepsilon_e)} \tag{A.2}$$

$$u_i^2 = \lambda^2 + \gamma_i^2; \ \gamma_i = \sqrt{i\omega\mu_0(\sigma_i + i\omega\varepsilon_i)} \tag{A.3}$$

Here, ω is wave angular frequency, ε is the dielectric permittivity, σ is electrical conductivity, μ_0 is the magnetic permeability, and subscripts 0, e and i refer to free space, electron and ion components, respectively. λ and γ denote real and imaginary (evanescent) components of wave numbers (not to be confused with wavelength λ_{air}).

For the geometry of Figure 1A.1 the exact integral expressions for the horizontal and radial components of the magnetic field as measured at the ground are

$$H_\phi = -\frac{\gamma_i m \cos\phi}{\pi\rho} \int_0^\infty \left(\frac{u_e}{u_0 + u_e}\right)\left(\frac{u_e}{u_0 + u_i}\right)\frac{J_1(\lambda\rho)\exp^{-u_0 h}}{D} d\lambda \tag{A.4}$$

$$H_\rho = \frac{\gamma_i m \sin\phi}{\pi}\left[\frac{1}{\rho}\int_0^\infty \left(\frac{u_e}{u_0 + u_e}\right)\left(\frac{u_e}{u_0 + u_i}\right)\frac{J_1(\lambda\rho)\exp^{-u_0 h}}{D} d\lambda \right.$$

$$\left. - \int_0^\infty \left(\frac{u_e}{u_0 + u_e}\right)\left(\frac{u_e}{u_0 + u_i}\right)\frac{\lambda J_0(\lambda\rho)\exp^{-u_0 h}}{D} d\lambda \right] \tag{A.5}$$

where

$$D = 1 - \left(\frac{u_0 - u_e}{u_0 + u_e}\right)\left(\frac{u_0 - u_i}{u_0 + u_i}\right)e^{-2u_0 h}, \tag{A.6}$$

and $J_0(x)$ and $J_1(x)$ are ordinary Bessel functions of the first kind. In these integral expressions the parameter λ plays the role of a dummy wave number integration variable.

To relate these exact expressions to the observations, the integrals are reduced according to several special cases over specified frequency ranges

- Special Case I

$|\gamma_e R| \gg 1 \, (R > 7\delta_e)$ and $|\gamma_e| \gg |\gamma_0|, \, |\gamma_i R| \gg 1 \, (R > 7\delta_i)$ and $|\gamma_i| \gg |\gamma_0|$

$$u_e \approx \gamma_e, \, \left(\frac{u_0 - u_e}{u_0 + u_e}\right) \approx -1, \, \frac{u_e}{u_0 + u_e} \approx 1$$

$$u_i \approx \gamma_e, \, \left(\frac{u_0 - u_i}{u_0 + u_i}\right) \approx -1, \, \frac{u_0}{u_0 + u_e} \approx \frac{u_0}{\gamma_i} \qquad (A.7)$$

$$\frac{e^{-u_0 h}}{D} \approx \frac{e^{-u_0 h}}{1 - e^{-2u_0 h}} = \frac{1}{2 \sinh u_0 h}$$

Then the integral expressions become

$$H_\phi \approx -\frac{m \cos \phi}{2\pi \rho} \int \frac{u_0 J_1(\lambda \rho)}{\sinh u_0 h} d\lambda \qquad (A.8)$$

$$H_\rho \approx \frac{m \sin \phi}{2\pi} \left[\frac{1}{\rho} \int_0^\infty \frac{u_0 J_1(\lambda \rho)}{\sinh u_0 h} d\lambda - \int_0^\infty \frac{u_0 \lambda J_0(\lambda \rho)}{\sinh u_0 h} d\lambda \right] \qquad (A.9)$$

where m is the equivalent magnetic dipole moment of the source. For the frequency range 4-2000 Hz of interest to HAARP studies, and for typical parameters for ionospheric conductivity and height, these general expressions may be further simplified.

Simplified Expressions 4-32 Hz

$$H_\phi \approx -\frac{m \cos \phi}{\pi d \rho^2} \left[\frac{d+h}{R_1} - \frac{h}{R} \right] G_i(u)$$

$$\qquad (A.10)$$

$$H_\rho \approx \frac{m \sin \phi}{\pi d} \left\{ \frac{1}{\rho^2} \left[\frac{d+h}{R_1} - \frac{h}{R} \right] G_i(u) + \left[\frac{d+h}{R_1^3} - \frac{h}{R^3} \right] V_i(u) \right\}$$

where

$$R^2 = \rho^2 + h^2, \, R_1^2 = \rho^2 + (d+h)^2 \qquad (A.11)$$

$$d = \frac{2}{\gamma_i} = \delta_i(1 - i), \, \delta_i \approx \sqrt{\frac{2}{\omega \mu_0 \sigma_i}} \qquad (A.12)$$

$$G_i(u) = \frac{u}{\pi} \coth u + \left(1 - \frac{1}{\pi}\right) u^2 \operatorname{csch}^2 u \qquad (A.13)$$

$$V_i(u) = u^3 \coth u \operatorname{csch}^2 u \qquad (A.14)$$

$$u = \frac{\pi \rho}{2h} \qquad (A.15)$$

42

Note: There is a null in H_ρ that occurs very near $\rho = h/\sqrt{2}$.

Limiting Cases:

- $\rho = 0$, directly beneath heated region

$$H_\phi \approx -\frac{m}{2\pi d h^2}\left[1 - \frac{h^2}{(d+h)^2}\right]\cos\phi$$

$$H_\rho \approx -\frac{m}{2\pi d h^2}\left[1 - \frac{h^2}{(d+h)^2}\right]\sin\phi$$

(A.16)

For $\rho \gg h$ (very great distance)

$$H_\phi \approx -\frac{m}{2\pi h \rho^2}\cos\phi$$

$$H_\rho \approx \frac{m}{2\pi h \rho^2}\sin\phi$$

(A.17)

Simplified Expressions for 64-1700 Hz

$$H_\phi \approx -\frac{m\cos\phi}{\pi R^3}\left(-\frac{i\pi x}{2}\right)H_1^{(2)}(x)\,f(x)\,G_i(u)$$

(A.18)

$$H_\rho \approx \frac{m\sin\phi}{\pi R^3}\left(-\frac{i\pi x}{2}\right)\left[G_i(u) - \left(\frac{3h^2}{R^2} - 1\right)\left(\frac{1+f(x)}{w}\right)V_i(u)\right]$$

(A.19)

where

$$x = 2\pi R/\lambda,\ f(x) = 1 - x\frac{H_0^{(2)}(x)}{H_1^{(2)}(x)},$$

(A.20)

and $H_{0,1}^{(2)}(x)$ are ordinary Hankel functions of the second kind. Here, λ is the wavelength, ϕ is the azimuthal angle measured counterclockwise from the horizontal electric dipole axis, and δ_i is the skin depth.

Limiting Cases:

$\rho = 0$, directly beneath the heated region

$$H_\phi \approx -\frac{m}{\pi h^3}K(x)\cos\phi \xrightarrow[x\gg 1]{} -\frac{i2\pi m}{(\lambda h)^{3/2}}\cos\phi$$

$$H_\rho \approx -\frac{m}{\pi h^3}K(x)\sin\phi \xrightarrow[x\gg 1]{} -\frac{i2\pi m}{(\lambda h)^{3/2}}\sin\phi$$

(A.21)

where

$$K(x) = -\frac{i\pi x}{2}H_1^{(2)}(x)f(x).$$

(A.22)

Fitting parameters are the height h of the source and the equivalent magnetic dipole moment m of the source. Observations of ELF intensities were made as a function of distance to HAARP and as a function of frequency. The amplitude of the signal was proportional to m, whereas the characteristic width/3 dB points relative to the minimum in the amplitude vs frequency curve, depend on the height of the source.